Catalysis
Science & Technology

Cite this: *Catal. Sci. Technol.*, 2012, **2**, 125–138

www.rsc.org/catalysis

PAPER

Exploring the versatility of a bis(phosphinimine) pincer ligand: effect of sterics on structure and lactide polymerization activity of cationic zinc complexes†

Craig A. Wheaton and Paul G. Hayes*

Received 6th August 2011, Accepted 10th September 2011
DOI: 10.1039/c1cy00306b

Cationic zinc complexes of a neutral pincer framework 4,6-(ArN=PPh$_2$)-dibenzofuran (**L^1**: Ar = 2-^{i}PrPh; **L^2**: Ar = *o*-tolyl; **L^3**: Ar = Ph), have been prepared and characterized. Crystallographic and NMR studies of the methylzinc complexes [LZnCH$_3^+$][BAr$_4^-$] (**4a–6a**: Ar = *m*-(CF$_3$)$_2$–C$_6$H$_3$; **4b–6b**: Ar = Ph) demonstrated that the steric demands of the ligand dramatically affect the solid-state geometry. The cationic zinc–lactate complexes [LZnOR$^+$][B(*m*-(CF$_3$)$_2$–C$_6$H$_3$)$_4^-$] (**7**: L = **L^2**; **8**: L = **L^3**; R = CH(Me)CO$_2$Me) were also studied, and their efficacy as lactide polymerization catalysts was examined. Polymerization using **7** requires heating to 60 °C, while complex **8** displays high activity at ambient temperature. The difference in activity can be attributed to κ^2 *versus* κ^3 binding modes of the ligand, providing important insight into structure–activity relationships for this system. Complex **8** gives modestly heteroenriched PLA (P_r = 0.70), which represents the best stereocontrol yet achieved by a cationic metal catalyst.

1. Introduction

The preparation of highly modular pincer-type ligands for the stabilization of reactive metal species is a topical field, whereby the properties of such ligands can be readily modified to suit the needs of various catalytic applications.[1,2] We have been exploring a neutral bis(phosphinimine) pincer architecture and coordinatively unsaturated cationic zinc complexes thereof, and have applied these compounds to the ring-opening polymerization of lactide (LA). It was expected that the electronically and coordinatively unsaturated metal centre would promote rapid monomer coordination, much like these properties promote rapid olefin polymerization in the well-known cationic metallocene catalysts of the early transition metals.[3] Polylactide (PLA) has seen increasing attention in recent years due to its potential viability as an eco-friendly commodity plastic which is biodegradable and sourced from renewable resources.[4] Many single-site catalysts for the controlled ring-opening polymerization of LA are known, and various reviews have been published.[5] These systems are typically neutral complexes supported by formally anionic ancillary ligands, and most commonly incorporate zinc,[6] magnesium,[7] calcium,[8] aluminium[9] (and the heavier group 13 metals[10]), and the rare earth metals.[11] Several cationic metal complexes have been employed for ring-opening polymerization of other lactones,[12] but there have only been a handful of reports of the application of such complexes for the polymerization of LA.[13] In general, these species have displayed poor activity or poorly defined structure of the active catalyst or the mechanism of polymerization. We have recently reported the first cationic metal complex capable of the controlled coordination-insertion polymerization of LA at ambient temperature.[14] Shortly thereafter, a cationic calcium complex was reported by Mountford *et al.* which also exhibits high activity at ambient temperature and excellent molecular-weight control.[13b]

Our initial foray into the field of LA polymerization catalysis utilized a mono(phosphinimine) architecture prepared by installation of a phosphinimine group on a dibenzofuran (dbf) backbone.[15] Zinc-alkyl complexes of this ligand exhibited bidentate coordination through the phosphinimine nitrogen and the dbf oxygen, but displayed relatively poor activity and control in polymerization experiments. However, substantially enhanced polymerization properties were achieved when a bis(phosphinimine) architecture, prepared by placement of phosphinimine moieties at the 4 and 6 positions of dibenzofuran, was employed.[16] Interestingly, the ligand was shown to coordinate zinc in a bidentate manner at the phosphinimine sites, with no participation of the dbf oxygen. More recently, we began probing the steric properties of this pincer system by replacing the 2,4,6-trimethylphenyl (Mes) *N*-aryl substituents with the less sterically demanding *para*-isopropylphenyl (Pipp) group. Cationic zinc complexes of this less encumbered system exhibited tridentate chelation. When an appropriate initiating group (methyl-lactate) was installed on zinc, this less bulky system proved to be an extremely active and living catalyst for

Department of Chemistry and Biochemistry, University of Lethbridge, E866 University Hall, 4401 University Drive, Lethbridge, Alberta, Canada. E-mail: p.hayes@uleth.ca; Fax: (+1) 403-329-2057
† CCDC reference numbers 833323–833330. For crystallographic data in CIF or other electronic format see DOI: 10.1039/c1cy00306b

the polymerization of *rac*-LA at ambient temperature.[14] Presently, it is not known whether this high activity is primarily due to decreased steric hindrance, or if the presence of the Zn–O bonding interaction also plays an important synergistic role.

In the current study, a wider investigation of the steric demands of the ancillary ligand has been undertaken, in hopes of obtaining a more complete understanding of structure–activity relationships for this novel class of cationic catalyst. Specifically, one *ortho* position of the *N*-aryl groups was left unsubstituted, while the substituent of the remaining *ortho* site was varied (H, CH_3, ^{i}Pr). We have prepared and studied the corresponding methylzinc complexes. Additionally, we have examined cationic zinc–lactate complexes in order to gauge the effect on lactide polymerization properties. All of the ligand variations employed have been found capable of stabilizing trigonal planar zinc cations, but significant variation in solid-state geometry, solution dynamics, and polymerization properties have been observed. The bulk of the ligand has been found to not only determine the binding mode (κ^2 or κ^3), but also the symmetry of the complex (C_s or C_2). Only the less bulky zinc–lactate complex, in which the ligand adopts a tridentate coordination mode, is a highly active polymerization catalyst at ambient temperature. Additionally, the catalyst generates modestly heterotactic enriched PLA (P_r = 0.70), representing the best stereochemical control yet achieved by a cationic catalyst system.

2. Results and discussion

2.1 Ligand synthesis

The ligands **L^1**–**L^3** were easily prepared from the diphosphine precursor and the appropriate aryl-azide, in isolated yields between 72.5–82.3%, giving analytically pure, thermally stable solids. All of the ligands exhibit similar features in the $^{31}P\{^1H\}$ NMR spectrum (C_6D_6 solvent), with each displaying one sharp singlet in the region between δ −6 and −4, suggesting C_{2v} symmetry in solution. The isopropyl groups of **L^1** appear in the expected regions in the ^{1}H NMR spectrum at δ 4.28 and 1.52, for the methine and methyl protons, respectively, while the characteristic *o*-tolyl methyl group of **L^2** resonates at δ 2.74. Single crystals suitable for X-ray diffraction were grown for each of these ligands, and their structures were verified by X-ray crystallography.†

2.2 Ligand protonation

We have exploited the same synthetic methodology used in our previous studies of cationic zinc[14–16] and magnesium species,[17] and in the preparation of cationic zinc complexes of a neutral α-diimine ligand by Bochmann *et al.*[12b,18] This route involves protonation of the ligand prior to complexation, thereby simultaneously installing a weakly coordinating anion while providing access to an efficient and irreversible alkane elimination pathway for complex preparation. As such, the complexes were readily prepared by reacting the protonated ligand with an appropriate alkyl-zinc precursor (Scheme 1). Brookhart's anion was installed using the oxonium acid reagent $[H(OEt_2)_2][B(C_6H_3(CF_3)_2)_4]$,[19] giving compounds **1a–3a**.

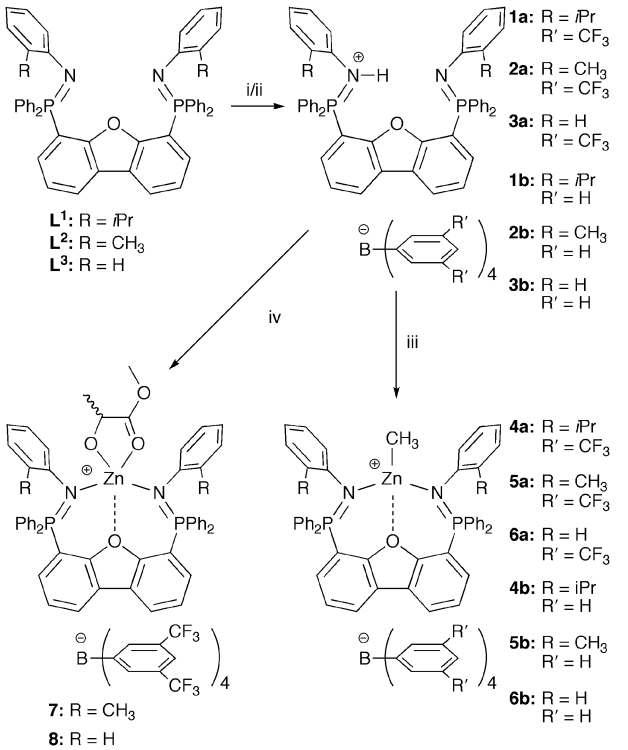

Scheme 1 Preparation of a series of cationic methylzinc and zinc–lactate complexes by first reacting the protonated ligand with (i) $[H(OEt_2)_2][B(C_6H_3(CF_3)_2)_4]$ (**1a–3a**) or (ii) HCl and $Na[BPh_4]$ (**1b–3b**) followed by reaction of the isolated protonated ligand with (iii) $ZnMe_2$ (**4–6**) or (iv) $EtZn(OCH(Me)CO_2Me)$ (**7**, **8**).

Additionally, the ligands were protonated using HCl, followed by reaction with sodium tetraphenylborate to install the BPh_4 counterion, giving compounds **1b–3b**. This counterion is less stable and prone to Ph transfer, but facilitates growth of single crystals and thereby expedites the solid-state characterization of the complexes. All protonated ligand derivatives were isolated in high yield (*ca.* 90% for **1a–3a**) as analytical pure powders, and are indefinitely stable at ambient temperature when stored under an inert atmosphere. As a general trend, introduction of the proton broadens the ^{1}H and $^{31}P\{^1H\}$ NMR signatures associated with the ligand, presumably as a result of inter- and intramolecular proton exchange between phosphinimine sites. Each protonated ligand displays only a single peak in the $^{31}P\{^1H\}$ NMR spectrum, suggesting that the proton exchange process is rapid on the NMR timescale, generating an average C_{2v} geometry in solution. As is usual for phosphinimine systems of this type, the protonation causes this resonance to shift downfield of the neutral ligand by approximately 20 ppm. The ^{31}P resonance appears between δ 14.3 and 19.2 for **1a–3a** (CD_2Cl_2), and between δ 12.6 and 14.5 for **1b–3b** (acetone-d_6). The acidic NH proton is difficult to observe in CD_2Cl_2 solvent, but is apparent as a broad singlet in the ^{1}H NMR spectra of **1b–3b** (acetone-d_6) between δ 4 and 5.

2.3 Cationic methylzinc complexes

Generation of the cationic methylzinc complexes **4a** and **4b** was easily achieved by reaction of $ZnMe_2$ with **1a** and **1b** (Scheme 1).

Surprisingly, compound **4b** was generated cleanly, with no evidence for back-transfer of a phenyl group from the anion. We attribute this observation to steric protection of the metal centre by the bulky isopropyl groups. The spectroscopic signatures of **4a** and **4b** are similar, with the organometallic methyl group appearing at δ −0.88. A single sharp peak appears in the $^{31}P\{^{1}H\}$ NMR spectrum at δ 22.7 (CD_2Cl_2), which is consistent with a tightly bound zinc cation in a left-right symmetric complex. The isopropyl CH_3 groups split into two resonances at δ 0.84 and 0.36 in the ^{1}H NMR spectrum, which we suggest is due to conformational rigidity of the complex and reduction of symmetry from C_{2v} to C_s (*vide infra*). This symmetry results in equivalent isopropyl groups, each with inequivalent methyls (Scheme 2). A variable-temperature ^{1}H NMR study was performed for **4a** (Fig. 1), and it was observed that the doublets morph into broad singlets at temperatures greater than 40 °C and coalesce to a single broad peak at 105 °C (C_6D_5Br). We propose that the coalescence of signals is due to a *syn–syn* fluxional process as displayed in Scheme 2, which has a calculated barrier $\Delta G^{\ddagger}$ = 18.0(2) kcal mol^{-1}.[20] The coalesced peak remains very broad at temperatures up to 120 °C, at which point significant decomposition of the compound becomes evident.

An X-ray crystal structure of complex **4b** has been obtained and is depicted in Fig. 2, with selected bond metrical data listed in Table 1. The zinc centre is κ^2 bound *via* the phosphinimine N-atoms, with no Zn–O_{dbf} interaction observed. The orientation of the ligand within complex **4b** is unique compared with previously studied analogues, whereby the N-aryl groups bend away from the binding pocket in the same direction, resulting in a *syn* orientation and a C_s-symmetric complex. Conversely, complexes of the previously studied mesityl substituted ligand adopted an *anti* conformation, rendering the zinc complex C_2-symmetric.[16] Furthermore, the previously studied Pipp-substituted ligand was established to be κ^3 bound due to the presence of a significant Zn–O_{dbf} interaction.[14] The *syn* orientation of the ligand in complex **4b** creates a rather sharp bite angle [N(1)–Zn(1)–N(2) = 113.30(5) Å], though the coordination geometry is best described as trigonal planar. The Zn–N distances average 2.053(1) Å, which is noticeably longer than the same bonds in the analogous complexes of $\mathbf{L^2}$ and $\mathbf{L^3}$ (*vide infra*). We suggest that this apparent weaker binding of the ligand is a result of the isopropyl groups, which sterically crowd the metal centre.

Reaction of dimethylzinc with the protonated ligands **2a** and **2b** rapidly afforded the desired methylzinc complexes **5a** and **5b**, respectively. Complex **5a** was isolated as an analytically pure powder in 97% yield. Unlike complexes **4** and **6** (*vide infra*), however, **5a** exhibits two relatively broad resonances in

Scheme 2 Proposed fluxional behaviour of **4a**, viewing down the plane of the dbf backbone (represented by the solid black line).

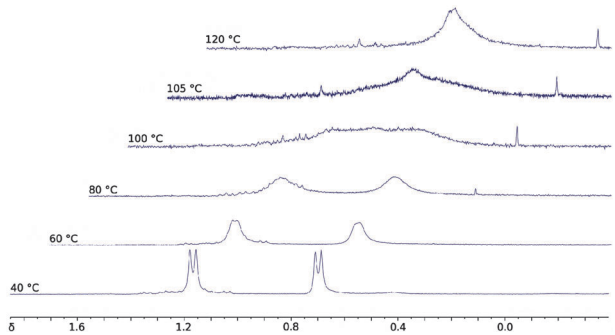

Fig. 1 Variable temperature ^{1}H NMR spectra of the isopropyl methyl groups of **4a**.

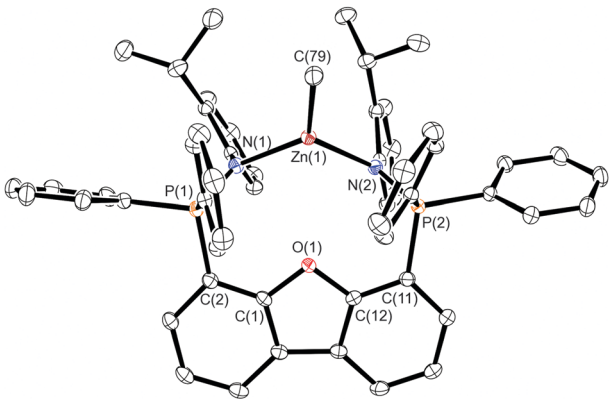

Fig. 2 Molecular structure of the cation of **4b**, with H-atoms omitted and ellipsoids drawn at the 30% probability level.

Table 1 Selected bond lengths (Å) and angles (°) from the crystal structures of **4b**, **5b**/**5c**, and **6b**/**6c**

	4b	**5b/c**	**6b/c**
Zn(1)–N(1)	2.050(1)	2.013(2)	2.004(2)
Zn(1)–N(2)	2.056(1)	2.020(2)	2.002(2)
Zn(1)–O(1)	3.125(1)	3.326(2)	3.276(2)
Zn(1)–C(x)	1.961(2)	1.967(4)	1.977(2)
P(1)–N(1)	1.601(1)	1.599(2)	1.601(2)
P(2)–N(2)	1.607(1)	1.602(2)	1.600(2)
N(1)–Zn(1)–N(2)	113.30(5)	124.20(9)	125.52(8)
N(1)–Zn(1)–C(x)[a]	123.67(7)	117.6(2)	116.12(8)
N(2)–Zn(1)–C(x)[a]	122.37(7)	118.2(2)	118.36(8)

[a] **4b**: x = 79; **5b**/**c**: x = 75; **6b**/**c**: x = 49.

the ambient temperature $^{31}P\{^{1}H\}$ NMR spectrum (δ 24.0 and 22.0 (C_6D_5Br)) in a 1 : 1 ratio. This is not due to inequivalent phosphinimines in the complex, but rather, arises from the presence of two distinct isomers, as indicated by two peaks (δ −0.39 and −0.84) in the ^{1}H NMR spectrum corresponding to the Zn–CH_3 moiety. This conclusion has been further corroborated by variable temperature NMR studies (Fig. 3), whereby it was found that the two peaks in the $^{31}P\{^{1}H\}$ NMR spectrum ($\Delta\nu_{max}$ = 327.6 Hz) coalesce to a single broad resonance at 56 °C. The energy barrier for this process was calculated to be $\Delta G^{\ddagger}$ = 15.0(1) kcal mol^{-1}. A concomitant coalescence and sharpening of the unique ^{1}H NMR resonances was also noted, with the Zn–CH_3 appearing at δ −0.40 (100 °C). Below ambient temperature, the NMR

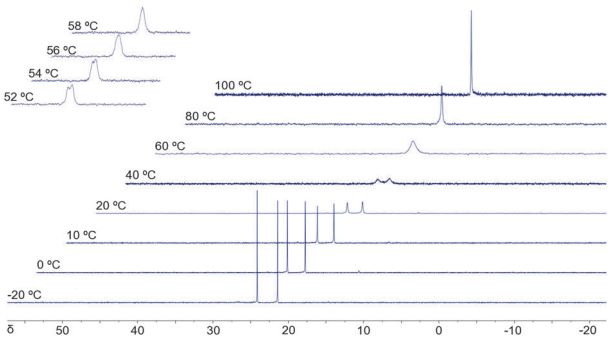

Fig. 3 Variable temperature $^{31}P\{^{1}H\}$ NMR spectra of compound **5a**.

signatures of both isomers sharpen substantially while maintaining a 1 : 1 ratio. We propose that these peaks correspond to *anti* (C_2) and *syn* (C_s) orientations of the ligand (Scheme 3). While the bulkier cations in **4a**/**4b** appear locked in a *syn* geometry, it would seem that reducing the steric constraints on the system significantly enhances flexibility, resulting in little energy difference between the two conformations.

The synthesis of **5b** from **2b** and $ZnMe_2$ does not proceed cleanly, giving rise to the phenylzinc species of the formula [L^2ZnPh][$MeBPh_3$] (**5c**) as a side product, in an approximate 60 : 40 ratio of **5b** : **5c**. Single crystals were obtained from the mixture of **5b** and **5c**, and X-ray diffraction studies showed the crystal contained the cations of both compounds in a ratio of approximately 3 : 1. Only a single independent unit of the ligand and the zinc centre exist, and the presence of both components was modelled as a substitutional disorder of the methyl and phenyl groups. The structure of **5b** is depicted in Fig. 4 with the disorder omitted for clarity; selected metrical parameters are presented in Table 1. The dbf ligand coordinates to the zinc centre *via* a κ^2 bonding mode, with no notable interaction between zinc and the dbf oxygen. The coordination geometry at zinc is thus best described as trigonal planar. The ligand adopts the *anti* orientation rather than the *syn* orientation observed for **4b**, and the complex is thereby *pseudo*-C_2-symmetric. The unsubstituted *ortho* positions of the *o*-tolyl groups are oriented toward the dibenzofuran backbone, while the methyl groups closely approach the coordination sphere of the zinc centre, providing a reasonable degree of steric protection. Compared with the previously studied mesityl analogue, which was also C_2-symmetric, the absence of a methyl group in the *ortho* site allows the ligand to adopt a sharper bite angle that is very close to ideal (120°).

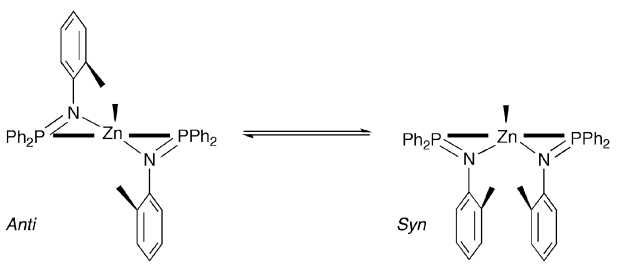

Scheme 3 Isomers of complex **5a**/**5b** with a view looking down the plane of the dbf backbone (represented by the solid black line).

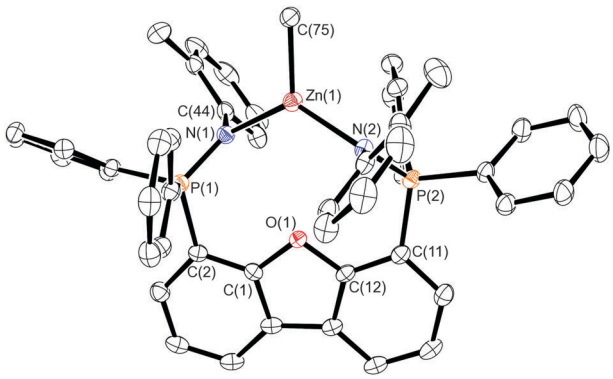

Fig. 4 X-Ray crystal structure of the cation of **5b**, with H-atoms omitted and ellipsoids drawn at the 30% probability level.

The synthesis of the cationic methylzinc complexes of L^3 (**6a** and **6b**) was performed similarly to **4** and **5**. The NMR spectra of **6a** are rather unremarkable, with the ZnMe moiety resonating at δ −1.02 in the ^{1}H NMR spectrum at ambient temperature. It is reasonable to suggest that interconversion between *anti* and *syn* isomers can occur in this complex even more readily than in complexes of L^2 because of the less imposing N-aryl group. However, no evidence of this fluxional process was observed at ambient temperature, suggesting rapid interconversion between isomers on the NMR timescale. Likewise, only one peak was observed in the $^{31}P\{^{1}H\}$ NMR spectrum.

Similarly to **5b**, the synthesis of compound **6b** was plagued by the production of an appreciable quantity (~20%) of the analogous phenylzinc compound [L^3ZnPh][$MeBPh_3$] (**6c**). Under the crystallization conditions employed, single crystals obtained from this mixture were enriched in the cation of **6c** (93%). Determination of the solid-state structure revealed a single molecule in the asymmetric unit, with the two compounds again modelled as a substitutional disorder of the phenyl and methyl groups. The X-ray crystal structure of the cation of **6c** is depicted in Fig. 5, while selected bond lengths and angles can be found in Table 2. Surprisingly, the ligand binds to the metal centre in a bidentate fashion, with no meaningful interaction between the dbf oxygen and zinc. The coordination geometry approaches trigonal planar. We attribute the lack of Zn–O_{dbf} bonding in this relatively non-hindered complex to packing effects in the solid-state, which necessarily suggests that the Zn–O_{dbf} interaction observed in the Pipp analogue[14] is relatively weak. The ligand geometry exists primarily in a *pseudo*-C_2-symmetric *anti* conformation. However, both phosphinimine groups exhibit significant disorder, with the minor component of each being in a *syn* conformation with respect to the major component of the other, lending support to the hypothesis that the complex undergoes rapid interconversion between *anti* and *syn* isomers in solution. This is modelled only as a positional disorder of the P and N atoms, in a ratio of 80 : 20 and 85 : 15 for P(1)–N(1) and P(2)–N(2), respectively.

2.4 Cationic zinc–lactate complexes

Complexes **4**–**6** are inactive for the polymerization of lactide, which is not surprising given our previous observation that cationic alkylzinc complexes are inefficient initiators.[14–16]

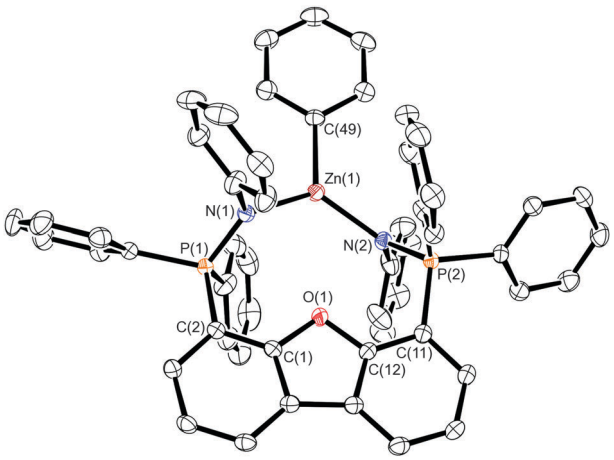

Fig. 5 Molecular structure of the cationic component of the by-product **6c** formed in the synthesis of **6b**, with H-atoms and disordered atomic positions omitted for clarity and ellipsoids drawn at the 30% probability level.

Table 2 Selected bond lengths [Å] and angles [°] from the crystal structures of complexes **7** and **8**

Bond	7	8	Angle	7	8
Zn(1)–N(1)	2.014(5)	2.016(3)	N(1)–Zn(1)–N(2)	124.8(2)	116.2(1)
Zn(1)–N(2)	1.996(4)	1.988(3)	N(1)–Zn(1)–O(3)	115.3(2)	122.3(1)
Zn(1)–O(1)	3.247(4)	2.367(2)	N(2)–Zn(1)–O(3)	118.6(2)	117.6(1)
Zn(1)–O(2)	2.105(4)	2.131(3)	O(3)–Zn(1)–O(2)	83.2(2)	83.3(1)
Zn(1)–O(3)	1.921(4)	1.904(3)	N(1)–Zn(1)–O(2)	99.6(2)	103.2(1)
P(1)–N(1)	1.599(4)	1.600(2)	N(2)–Zn(1)–O(1)	N/A	83.7(1)
P(2)–N(2)	1.593(5)	1.597(4)	O(1)–Zn(1)–O(2)	N/A	168.3(1)

Therefore, in order to probe the effects of ligand structure on LA polymerization, it was necessary to install a suitable initiating group. This was accomplished by reaction of HL^+ with EtZn(OCH(Me)CO_2Me) to generate the corresponding methyl-lactate zinc complexes. The methyl-lactate moiety is an excellent initiating group, in addition to being a very close structural mimic of the growing polymer chain. Thus, studies of such complexes provide a great deal of insight into the nature of the active catalyst species. The synthesis of these complexes required rather harsh conditions relative to preparation of the related methylzinc compounds, and therefore the tetraphenylborate anion could not be employed. Additionally, the synthetic methodology proved ineffective for the most sterically hindered ligand $\mathbf{L^1}$. For this reason, only zinc–lactate complexes of $\mathbf{L^2}$ and $\mathbf{L^3}$ were prepared and studied.

Reaction of **2a** or **3a** with racemic EtZn(methyl-DL-lactate) for a period of 1 h at 100 °C cleanly afforded complexes **7** and **8**, respectively. Each was isolated as a thermally stable, analytically pure white crystalline solid in good yield (**7**: 76%, **8**: 72%). Compound **7** displays fluxional solution behaviour similar to the methylzinc complex of $\mathbf{L^2}$, with broad resonances appearing in the ^{1}H NMR spectrum. However, instead of two distinct isomers, the ambient temperature $^{31}P\{^1H\}$ NMR spectrum displayed three broad resonances of approximately equal intensity at δ 27.0, 26.6, and 26.0. These signals coalesce to a single broad resonance at 60 °C, corresponding to an activation barrier of approximately $\Delta G^{\ddagger} = 16$ kcal mol^{-1} (Fig. 6).[21] This peak sharpens considerably at elevated temperatures, giving a singlet at δ 27.2 at 80 °C. The ^{1}H NMR spectrum also exhibits sharp signals at this temperature with characteristic methyl-lactate peaks observed at δ 4.39 (methine), 2.89 (OMe), and 1.35 (CMe).[22] At temperatures below 20 °C, the NMR spectra suffer from substantial broadening, but at −20 °C the $^{31}P\{^1H\}$ NMR spectrum simplifies into predominantly two relatively sharp peaks at δ 26.7 and 25.7. The presence of three isomers is readily explained by considering the symmetry of the ligand in the *anti* and *syn* orientations and how these interact with the asymmetric methyl-lactate moiety (Scheme 4). When the ligand exists in the C_2-symmetric orientation, two unique diastereomers can be distinguished for a given methyl-lactate enantiomer (*anti*-A and *anti*-B), while for the C_s-symmetric orientation only a single diastereomer is possible (*syn*). For the opposite enantiomer of the methyl-lactate moiety the resulting isomers are enantiomers of the former.

In contrast, the NMR spectra of complex **8** are relatively straightforward, including a single peak in the $^{31}P\{^1H\}$ spectrum at δ 29.3. However, examination of the ^{1}H NMR spectrum suggests two unique isomers, as evidenced by two distinct sets of resonances. Specifically, resonances attributed to the methyl-lactate moiety appear at δ 3.42 (C*H*(CH$_3$)), 3.44 (OC*H*$_3$) and 0.87 (CH(C*H*$_3$)), while a second set of equally intense signals resonate at δ 4.07, 3.93 and 1.36 (CD_2Cl_2). The identity of these isomers is presently unknown, but may be related to the relative positions of the two coordinating methyl-lactate oxygen atoms with respect to axial and equatorial trigonal bipyramidal sites (*vide infra*).

High quality single crystals of complexes **7** and **8** suitable for X-ray diffraction were obtained and their solid-state structures are depicted in Fig. 7 and 8, respectively. Selected metrical parameters are located in Table 2.

Interestingly, the structure of **7** finds $\mathbf{L^2}$ in the *syn*, as opposed to the *anti* conformation observed in the solid-state structure of **5b**. The ancillary ligand is κ^2 bound, as there is no evidence for a substantive Zn–O_{dbf} interaction. Thus, the zinc centre is 4-coordinate with a geometry that is best described as trigonal pyramidal. The equatorial sites are occupied by the phosphinimine donors and the formally anionic oxygen atom (O(3)) of the lactate group, with bond lengths in the expected ranges, and a sum of angles about these equatorial sites of 358.7(3)°. The bite angle of the ligand in this *pseudo*-C_s-symmetric complex is 124.8(2)°, which is similar to that of the C_2-symmetric ligand in the analogous methylzinc

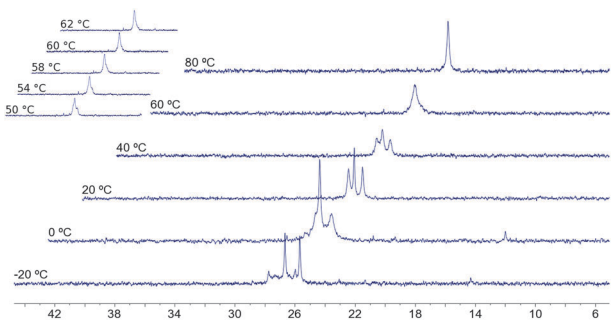

Fig. 6 Variable temperature $^{31}P\{^1H\}$ NMR spectra of complex **7**.

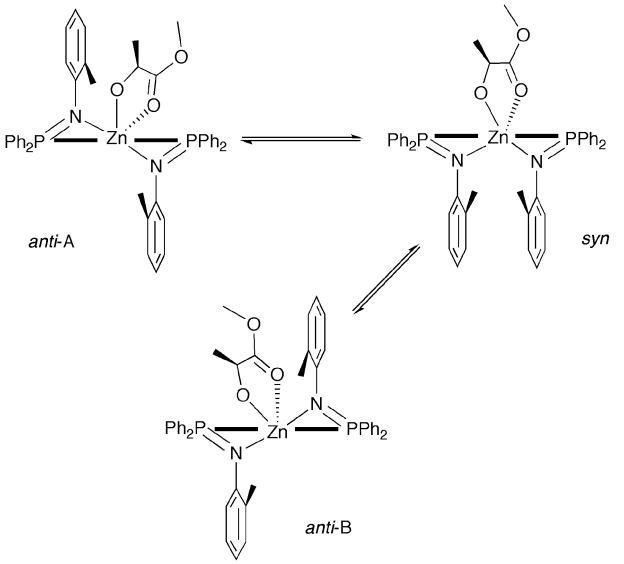

Scheme 4 Possible isomers of complex **7** for a methyl-D-lactate moiety, with a view down the plane of the dbf backbone (represented by a solid black line).

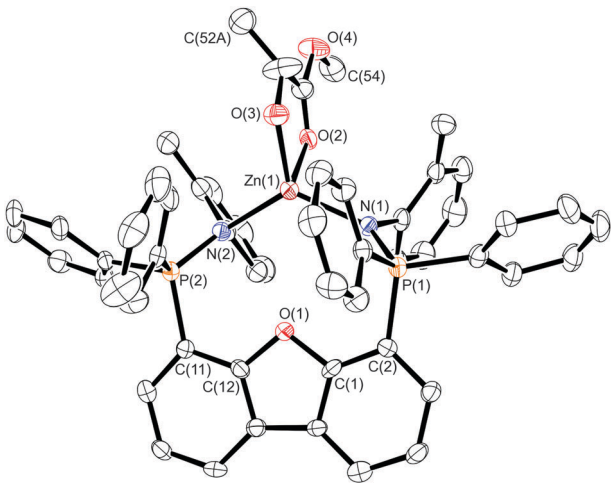

Fig. 7 Molecular structure of the cation of **7**, with H-atoms omitted and ellipsoids drawn at the 30% probability level.

complex **5b**. Although there is only one independent molecule in the unit cell, the compound is a racemic mixture, which has been modelled as a positional disorder of the methyl group C(52).

The X-ray crystal structure of complex **8** shows major differences compared with that of **7**, despite the seemingly small change in the ligand. Specifically, the ligand is κ^3 bound to the zinc centre, whereby a significant Zn–O_{dbf} interaction occurs (Zn(1)–O(1) = 2.367(2) Å). This results in a zinc coordination geometry that is similar to the structure of the analogous complex of the Pipp ligand previously reported.[14] Use of Addison and Reedijk's trigonality parameter[23] gave $\tau = 0.72$, suggesting a primarily trigonal bipyramidal coordination geometry. The equatorial sites are occupied by the phosphinimine N-donors and O(3), with a sum of angles about these sites of 356.1(2)°. The weaker, formally neutral oxygen donors occupy the axial sites at an angle of 168.3(1)°. As in

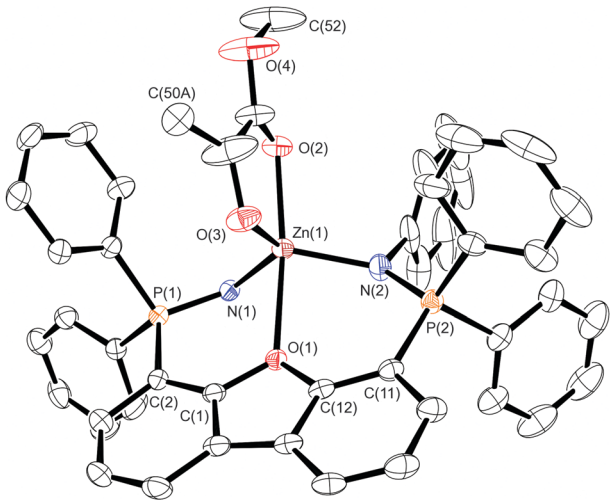

Fig. 8 Molecular structure of the cation of **8**, with hydrogen atoms and an N-phenyl omitted for clarity and ellipsoids drawn at the 30% probability level.

complex **7**, the compound is a racemic mixture, which is modelled as a position disorder of C(50).

2.5 Polymerization studies

Preliminary studies of the performance of complexes **7** and **8** as LA polymerization catalysts have been performed in order to establish the effect of ligand bulk and coordination mode. Compound **7** shows little activity for polymerization of *rac*-LA at ambient temperature, and must be heated to 60 °C to achieve polymerization at a reasonable rate. In $CDCl_3$ solvent at 60 °C, with an initial monomer concentration of 1 M and a catalyst loading of 0.5 mol% ($[LA]_0/[7] = 200$), polymerization occurs under well-behaved first-order kinetics with an observed rate constant of $3.65(2) \times 10^{-4}$ s^{-1} (Table 3). This rate is only slightly better than that observed for the bulkier mesityl substituted complex previously reported, despite the significant reduction in steric bulk.[16] Analysis of the stereochemistry of isolated polymer samples revealed slight stereocontrol and a modestly heteroenriched polymer chain ($P_r = 0.61$).[24] Gel permeation chromatography (GPC) of the same isolated polymer sample indicated reasonably good molecular weight control. The number-average molecular weight (M_n) was 18.0×10^3 g mol^{-1}, and the polydispersity was 1.37. Furthermore, MALDI-ToF mass spectra of the polymer were obtained, which support a coordination-insertion mechanism, as the mass of all polymer peaks are consistent with a methyl-lactate end group. However, mass peaks are separated by $m/z = 72$, which suggests appreciable transesterification side-reactions.

Table 3 Observed rates of polymerization of *rac*-lactide by three cationic zinc–lactate complexes[a]

	Temp. (°C)	$[LA]_0/[Zn]$	Solvent	k_{obs} ($\times 10^{-4}$ s^{-1})
7	60	200	$CDCl_3$	3.65(2)
8	25	200	CD_2Cl_2	5.11(3)
Pipp analogue[14]	25	200	CD_2Cl_2	8.65(4)

While complex **8** may appear to be only marginally less sterically encumbered than catalyst **7**, it was found to be dramatically more active for the polymerization of *rac*-LA. Complex **8** displayed high activity at ambient temperature, and in CH_2Cl_2 solvent the observed first-order rate constant at 25 °C was determined to be $5.11(3) \times 10^{-4}$ s^{-1}. Interestingly, this rate is somewhat slower than that established for the previously studied Pipp analogue under identical conditions ($8.65(4) \times 10^{-4}$ s^{-1}), despite their similar steric bulk (Table 3). As such, the moderate reduction in activity cannot simply be attributed to steric differences, and we therefore propose that electronic effects are responsible. The lack of a *para*-isopropyl group on the N-aryl rings somewhat reduces the electron donating capacity of the ligand, thereby rendering the zinc centre in **8** slightly more electropositive. Thus, the activity of these catalysts is highly dependent on the electrophilicity of the metal centre, and suggests that better moderation of electron density may lead to improved activity. Hence, we conclude that the reason for the large difference in activity between **7** and **8**, which is not commensurate with the difference in steric bulk, is due largely to the difference in the coordination geometry of the ligand. Specifically, the interaction between the cationic zinc centre and the dbf oxygen, that is only present in sterically open complexes (**8** and the Pipp analogue) is strong enough to help moderate the electrophilicity of the metal. We thus conclude that reduced steric demand of the ligand with concomitant reduction in metal electrophilicity work synergistically to promote enhanced LA polymerization activity in cationic zinc complexes stabilized by dbf-based bis(phosphinimine) pincer ligands.

Analysis of polymer samples produced using **8** as catalyst showed very similar properties compared with those generated using **7**. At ambient temperature under otherwise identical conditions, the molecular weight was found to be 18.9×10^3 g mol^{-1}, and the molecular weight distribution low (PDI = 1.35). However, analysis of the tetrad sequences revealed significantly enhanced stereocontrol, with isolated polymer samples exhibiting substantial heterotactic enrichment (P_r = 0.70), presumably due to a chain-end control mechanism.[25] This level of stereoregularity is uncommon for zinc catalysts active at ambient-temperature, and represents the best stereocontrol yet reported for polymerization of *rac*-lactide by a cationic metal complex.

3. Conclusions

In summary, a series of closely related bis(phosphinimine) ligands, $\mathbf{L^1}$–$\mathbf{L^3}$, which differ only in the nature of the substituents in the *ortho* positions of N-aryl groups, have been constructed from a dibenzofuran backbone. Cationic methylzinc complexes of each ligand were prepared and structurally characterized. All species were found to have low-coordinate trigonal planar geometry, and exist as well separated ion pairs. The structural investigations established that the bulkiness of the N-aryl groups has a substantial impact on ligand orientation in the complexes.

The synthesis of zinc–lactate complexes was only possible using the two less bulky ligands ($\mathbf{L^2}$ and $\mathbf{L^3}$). These complexes were fully characterized and their efficacy for polymerization of *rac*-LA was explored. Notably, polymerization activity is heavily dependent upon the steric bulk of the ancillary ligand; removal of only a single methyl substituent from each N-aryl group resulted in a dramatic improvement in activity. This increased activity is attributed not only to the reduced steric constraints, but also to the additional stabilizing interaction between zinc and the dibenzofuran oxygen, which occurs only within the less bulky complex. The study has thus significantly advanced our knowledge of fundamental structure–activity relationships, which will allow further rational development of this relatively new pincer ligand, whereby catalytic activity and control may be simultaneously optimized. Remarkably, complex **8** also displays improved stereoselectivity, giving substantially heteroenriched PLA (P_r = 0.70), which is unprecedented for well-defined cationic metal complexes.

4. Experimental section

4.1 General procedures

All manipulations of air-sensitive materials and reagents were conducted using high-vacuum techniques under a purified argon atmosphere or in a glove box (MBraun Labmaster 130). Protio solvents were purified using an MBraun solvent purification system (MB-SPS), stored in Teflon-sealed glass vessels over appropriate drying agents, and vacuum transferred directly to reaction vessels. Deuterated solvents (Cambridge Isotopes) were dried with appropriate drying agents, vacuum transferred, and stored under an inert atmosphere prior to use. All other materials were obtained in high purity (Sigma-Aldrich, Acros Organics) and used without additional purification. NMR spectra (^{1}H (300.13 MHz), ^{13}C{^{1}H} (75.47 MHz), ^{31}P{^{1}H} (121.48 MHz), ^{19}F (282.42 MHz), and ^{11}B (96.29 MHz)) were collected using a Bruker Avance II NMR spectrometer equipped with a variable-temperature unit. Spectra were collected at ambient temperature and referenced to residual solvent resonances (^{1}H and ^{13}C{^{1}H}), or an external standard (triphenylphosphine (^{31}P{^{1}H}), trifluorotoluene (^{19}F), or boron trifluoride diethyl etherate (^{11}B)). ^{1}H and ^{13}C NMR peak assignments were facilitated by DEPT, COSY, and HSQC experiments. X-ray crystal structures were collected using a Bruker AXS SMART APEX II single crystal X-ray diffractometer (Mo-Kα (λ = 0.71073 Å)). Elemental analyses were performed using an Elementar Vario Microcube. MALDI mass spectra were performed on an ultraflexXtreme™ MALDI-TOF/TOF (Bruker Daltonics, Billerica, MA, USA) mass spectrometer in positive MS mode using 2-[(2*E*)-3-(4-*tert*-butylphenyl)-2-methylprop-2-enylidene]malononitrile (DCTB) as the matrix compound. GPC data were obtained on a Varian PL-GPC 50 Plus instrument and measured against polystyrene standards. The molecular weight values were scaled by the accepted Mark-Houwink parameter of 0.58.[26] Phenyl-azide[27] and 2-isopropylphenyl-azide[28] were prepared according to published literature procedures,[29] and the spectral data match literature values. The ligand diphosphine precursor was prepared by the previously reported procedure.[30]

4.2 Details of polymerization studies

In situ. In a glovebox, an NMR tube was loaded with an appropriate amount of catalyst (4.0 mg for $[LA]_0/[\mathbf{2}]$ = 200)

and 72.1 mg of *rac*-LA, to which 0.50 mL of cold (−35 °C) $CDCl_3$ (**7**) or CD_2Cl_2 (**8**) was then added. The tube was immediately sealed with a rubber septum, removed from the glove box, cooled to −78 °C in dry ice, and transported to a temperature stabilized (60 °C for **7** and 25 °C for **8**) and pre-shimmed NMR instrument. The tube was then allowed to warm and was inserted into the probe after complete dissolution of the *rac*-LA was observed. Measurements were begun immediately thereafter.

Preparation of polymer samples. Using **8** as catalyst: In a glove box with an ambient temperature of approximately 25 °C, a scintillation vial was loaded with 144.1 mg (1.0 mmol) of *rac*-LA and 8.8 mg (0.0050 mmol) of **8**. To the vial 1 mL of CH_2Cl_2 was added and the resulting solution was stirred for 75 min. The solution was exposed to air and 10 mL of cold methanol (−35 °C) was added. The polymer was isolated by centrifugation, redissolved in 1 mL of CH_2Cl_2 and reprecipitated once more with cold methanol. The isolated polymer sample was dried exhaustively *in vacuo*, yielding 139 mg (∼96%). Polymer preparation using **7** as catalyst was performed at 40 °C over 8 h under otherwise similar conditions, yielding 130 mg of polymer (∼90%).

4.3 Synthesis and characterization

***o*-Tolyl-azide (*o*-Tol-N_3).** The standard methodology for azide preparation was employed,[29] giving a yellow liquid in 81% yield (12.2 g, 0.0916 mol). ^{1}H NMR ($CDCl_3$): δ 7.22 (t, 1H, $^3J_{HH}$ = 7.5 Hz, 3-*o*-Tol), 7.15 (d, 1H, $^3J_{HH}$ = 7.5 Hz, 4-*o*-Tol), 7.10 (d, 1H, $^3J_{HH}$ = 7.6 Hz, 1-*o*-Tol), 7.03 (d, 1H, $^3J_{HH}$ = 7.6 Hz, 2-*o*-Tol), 2.21 (s, 3H, CH_3); ^{13}C{^{1}H} NMR ($CDCl_3$): δ 138.53 (s, 6-*o*-Tol), 131.30 (s, 4-*o*-Tol), 129.74 (s, 5-*o*-Tol), 127.25 (s, 3-*o*-Tol), 124.74 (s, 2-*o*-Tol), 118.05 (s, 1-*o*-Tol), 17.40 (s, CH_3).

4,6-(2-^{i}PrPh–N=PPh_2)$_2$-dbf (L^1). In a 100 mL round bottom flask attached to a swivel-frit apparatus, 4,6-bis(diphenylphosphino)dibenzofuran (1.00, 1.86 mmol) was dissolved in toluene (40 mL). 2-isopropylphenyl-azide (0.63 g, 3.9 mmol) was added, and the resulting solution was stirred for 18 h at a temperature of 70 °C. After cooling to ambient temperature, the solution was filtered through the frit to remove any trace undissolved impurities, and was then concentrated to a volume of 5 mL. To this 30 mL of pentane was added, causing precipitation of the product as a yellow powder. Vigorous stirring for 1 h produced a fine yellow powder, which was collected by filtration, washed with pentane (3 × 5 mL), and dried under vacuum. Yield: 1.08 g (1.35 mmol), 72.5%. ^{1}H NMR (C_6D_6): δ 8.26 (dd, 2H, $^3J_{PH}$ = 13.6 Hz, $^3J_{HH}$ = 6.4 Hz, 3,7-H dbf), 7.64 (dd, 8H, $^3J_{PH}$ = 12.8 Hz, $^3J_{HH}$ = 7.0 Hz, *o*-Ph), 7.49 (d, 2H, $^3J_{HH}$ = 7.7 Hz, 1,9-H dbf), 7.37 (m, 2H, 4-NAr), 7.00–6.80 (ov m, 10H, *p*-Ph + 2,8-H dbf + 2-NAr + 3-NAr), 6.73 (td, 8H, $^3J_{HH}$ = 7.6 Hz, $^4J_{PH}$ = 3.0 Hz, *m*-Ph), 6.63 (m, 2H, 1-NAr), 4.28 (sp, 2H, $^3J_{HH}$ = 6.9 Hz, $CH(CH_3)_2$), 1.52 (d, 12H, $^3J_{HH}$ = 6.9 Hz, $CH(CH_3)_2$); ^{31}P{^{1}H} NMR (C_6D_6): δ −5.2 (s); ^{13}C{^{1}H} NMR (C_6D_6): δ 156.76 (d, J = 2.6 Hz), 149.07 (d, J = 1.1 Hz), 143.28 (d, $^2J_{CP}$ = 21.7 Hz), 135.06 (d, $^2J_{CP}$ = 6.6 Hz, 3,7-dbf), 132.66 (d, $^3J_{CP}$ = 10.2 Hz, *o*-Ph), 131.94 (d, $^1J_{CP}$ = 107.6 Hz, *ipso*-Ph), 131.83 (d, $^4J_{CP}$ = 2.9 Hz, *p*-Ph), 129.02 (d, $^3J_{CP}$ = 12.6 Hz, *m*-Ph), 126.44 (s, 3-NAr), 126.18 (d, $^4J_{CP}$ = 2.2 Hz, 4-NAr), 125.14 (dd, J_{CP} = 6.3 Hz, J_{CP} = 0.9 Hz), 125.00 (d, $^4J_{CP}$ = 2.5 Hz, 1,9-dbf), 124.35 (d, $^3J_{CP}$ = 9.9 Hz, 2,8-dbf), 121.78 (d, $^3J_{CP}$ = 10.1 Hz, 1-NAr), 118.90 (d, $^4J_{CP}$ = 0.5 Hz, 2-NAr), 117.60 (d, $^1J_{CP}$ = 85.6 Hz, 4,6-dbf), 29.20 (s, $CH(CH_3)_2$), 23.70 (s, $CH(CH_3)_2$); elemental analysis calcd (%) for $C_{54}H_{48}N_2OP_2$: C 80.78, H 6.03, N 3.49; found: C 80.48, H 6.03, N 3.29.

4,6-(*o*-Tol-N=PPh_2)$_2$-dbf (L^2). L^2 was prepared similarly to L^1 from 4,6-bis(diphenylphosphino)dibenzofuran (1.00 g, 1.86 mmol) and *o*-tol-N_3 (0.52 g, 3.90 mmol), affording L^2 as a light yellow powder in 80.6% yield (1.12 g, 1.50 mmol). ^{1}H NMR (C_6D_6): δ 8.27 (dd, 2H, $^3J_{PH}$ = 13.4 Hz, $^3J_{HH}$ = 7.6 Hz, 3,7-H dbf), 7.64 (dd, 8H, $^3J_{PH}$ = 12.7 Hz, $^3J_{HH}$ = 7.4 Hz, *o*-Ph), 7.49(d, 2H, $^3J_{HH}$ = 7.6 Hz, 1,9-dbf), 7.32(d, 2H, $^3J_{HH}$ = 7.0 Hz, 4-*o*-Tol), 6.95 (t, 2H, $^3J_{HH}$ = 7.6 Hz, 2,8-dbf), 6.92–6.85 (ov m, 6H, *p*-Ph + 2-*o*-Tol), 6.81 (2H, $^3J_{HH}$ = 7.1 Hz, 3-*o*-Tol), 6.74(td, 8H, $^3J_{HH}$ = 7.6 Hz, $^4J_{PH}$ = 2.8 Hz, *m*-Ph), 6.58(d, 2H, $^3J_{HH}$ = 7.7 Hz, 1-*o*-Tol), 2.74 (s, 6H, CH_3 *o*-Tol); ^{31}P{^{1}H} NMR (C_6D_6): δ −5.9; ^{13}C{^{1}H} NMR (C_6D_6): δ 156.80 (d, J_{CP} = 2.6 Hz), 150.30 (d, J_{CP} = 1.0 Hz), 135.02 (d, $^2J_{CP}$ = 6.5 Hz, 3,7-dbf), 133.47 (d, J_{CP} = 22.4 Hz), 132.67 (d, $^2J_{CP}$ = 10.2 Hz, *o*-Ph), 131.96 (d, $^1J_{CP}$ = 106.8 Hz, *ipso*-Ph), 131.85 (d, $^4J_{CP}$ = 3.0 Hz, *p*-Ph), 131.03 (d, $^4J_{CP}$ = 2.0 Hz, 4-*o*-Tol), 129.02 (d, $^3J_{CP}$ = 12.5 Hz, *m*-Ph), 126.83 (s, 2-*o*-Tol), 125.10 (dd, J_{CP} = 6.5 Hz, J_{CP} = 0.9 Hz), 125.00 (d, $^4J_{CP}$ = 2.3 Hz, 1,9-dbf), 124.30 (d, $^3J_{CP}$ = 10.2 Hz, 2,8-dbf), 121.28 (d, $^3J_{CP}$ = 9.7 Hz, 1-*o*-Tol), 118.52 (s, 3-*o*-Tol), 117.52 (d, $^1J_{CP}$ = 87.4 Hz, 4,6-dbf), 20.62 (s); elemental analysis calcd (%) for $C_{50}H_{40}N_2OP_2$: C 80.41, H 5.40, N 3.75; found: C 80.34, H 5.31, N 3.78.

4,6-(Ph–N=PPh_2)$_2$-dbf (L^3). L^3 was prepared similarly to L^1 from 4,6-bis(diphenylphosphino)dibenzofuran (1.00 g, 1.86 mmol) and phenyl-azide (0.47 g, 3.95 mmol). This reaction was much more facile; reaction at ambient temperature for a 2 h period proved sufficient to give complete conversion of the phosphine starting material, affording L^3 as a pale yellow powder in 82.3% yield (1.10 g, 1.53 mmol). ^{1}H NMR (C_6D_6): δ 8.24 (dd, 2H, $^3J_{PH}$ = 13.9 Hz, $^3J_{HH}$ = 7.6 Hz, 3,7-dbf), 7.68 (dd, 8H, $^3J_{PH}$ = 12.6 Hz, $^3J_{HH}$ = 7.6 Hz, *o*-Ph), 7.48 (d, 2H, $^3J_{HH}$ = 7.6 Hz, 1,9-dbf), 7.18–7.04 (ov m, 8H, *o* + *m*-NPh), 6.98–6.88 (ov m, 6H, *p*-Ph + 2,8-dbf), 6.87–6.75 (ov m, 10H, *m*-Ph + *p*-NPh); ^{31}P{^{1}H} NMR (C_6D_6): δ −4.2 (s); ^{13}C{^{1}H} NMR (C_6D_6): δ 156.86 (d, J_{CP} = 2.2 Hz), 152.08 (d, J_{CP} = 1.9 Hz), 134.92 (d, $^2J_{CP}$ = 7.1 Hz, 3,7-dbf), 132.92 (d, $^2J_{CP}$ = 10.2 Hz, *o*-Ph), 131.87 (d, $^4J_{CP}$ = 3.0 Hz, *p*-Ph), 131.67 (d, $^1J_{CP}$ = 103.7 Hz, *ipso*-Ph), 129.54 (d, $^4J_{CP}$ = 1.2 Hz, *m*-NPh), 129.06 (d, $^3J_{CP}$ = 12.4 Hz, *m*-Ph), 125.14 (dd, J_{CP} = 6.4 Hz, J_{CP} = 0.9 Hz), 124.96 (d, $^4J_{CP}$ = 2.5 Hz, 1,9-dbf), 124.42 (d, $^3J_{PC}$ = 17.8 Hz, *o*-NPh), 124.14 (d, $^3J_{PC}$ = 10.4 Hz, 2,8-dbf), 118.42 (d, $^5J_{PC}$ = 0.8 Hz, *p*-NPh), 116.96 (d, $^1J_{CP}$ = 93.0 Hz, 4,6-dbf); Elemental analysis calcd (%) for $C_{48}H_{36}N_2OP_2$: C 80.21, H 5.05, N 3.90; found: C 80.23, H 5.30, N 3.48.

[L^1H^+][$B(C_6H_3(CF_3)_2)_4^-$] (**1a**). The ligand $\mathbf{L^1}$ (200 mg, 0.249 mmol) and the oxonium acid $[H(OEt_2)_2][B(C_6H_3(CF_3)_2)_4]$ (252 mg, 0.249 mmol) were combined in a glass vial. To the vial 2 mL of benzene was added, and the mixture was stirred for several min until all material was dissolved, giving a clear red/orange solution. This mixture was allowed to stand for 5 min, and then 5 mL of pentane was added to precipitate the product as a red/orange oil. The supernatant was decanted, the oil was washed with pentane (3 × 1 mL) and dried *in vacuo* giving the product as a light yellow powder in 88.4% yield (367 mg, 0.220 mmol). ^{1}H NMR (CD_2Cl_2): δ 8.46 (d, 2H, $^3J_{HH}$ = 7.7 Hz, 1,9-dbf), 7.74 (br s, 8H, *o*-BAr^F_4), 7.64 (td, 2H, $^3J_{HH}$ = 7.7 Hz, $^4J_{PH}$ = 2.4 Hz, 2,8-dbf), 7.56 (br s, 4H, *p*-BAr^F_4), 7.50 (tt, 4H, $^3J_{HH}$ = 7.5 Hz, $^4J_{HH}$ = 3.1 Hz, *p*-Ph), 7.39 (dd, $^3J_{PH}$ = 11.6 Hz, $^3J_{HH}$ = 7.7 Hz, 3,7-dbf), 7.36–7.21 (ov m, 16H, *o*-Ph + *m*-Ph), 7.08 (d, 2H, $^3J_{HH}$ = 7.6 Hz, 4-NAr), 6.88 (t, 2H, $^3J_{HH}$ = 7.6 Hz, 3-NAr), 6.42 (t, 2H, $^3J_{HH}$ = 7.6 Hz, 2-NAr), 6.16 (d, 2H, $^3J_{HH}$ = 7.6 Hz, 1-NAr), 3.19 (sp, 2H, $^3J_{HH}$ = 6.9 Hz, $CH(CH_3)_2$), 0.94 (d, 12H, $^3J_{HH}$ = 6.9 Hz, $CH(CH_3)_2$). The acidic NH proton was not observed. $^{31}P\{^1H\}$ NMR (CD_2Cl_2): δ 15.8 (br s); $^{19}F\{^1H\}$ NMR (CD_2Cl_2): δ 61.9 (s); $^{11}B\{^1H\}$ NMR (CD_2Cl_2): δ −6.6 (s); $^{13}C\{^1H\}$ NMR (CD_2Cl_2): δ 162.32 (q, $^1J_{BC}$ = 49.9 Hz, *ipso*-BAr^F_4), 158.15 (d, J_{PC} = 1.8 Hz, Aromatic C), 145.88 (d, J_{PC} = 10.6 Hz, Aromatic C), 135.36 (br s, *o*-BAr^F_4), 134.93 (br s, *p*-Ph), 133.83 (d, $^2J_{PC}$ = 6.6 Hz, 3,7-dbf), 133.10 (d, $^2J_{PC}$ = 10.4 Hz, *o*-Ph), 129.89 (d, $^3J_{PC}$ = 13.2 Hz, *m*-Ph), 129.43 (qq, $^2J_{FC}$ = 31.5 Hz, $^3J_{BC}$ = 2.9 Hz, *m*-BAr^F_4), 128.86 (s, Aromatic C), 128.37 (s, 1,9-dbf), 127.05 (d, $^4J_{PC}$ = 2.0 Hz, 2-NAr), 126.80 (s, 4-NAr), 125.62 (d, $^3J_{PC}$ = 5.8 Hz, 1-NAr), 125.55 (d, $^3J_{PC}$ = 9.8 Hz, 2,8-dbf), 125.33 (br s, 3-NAr), 125.14 (q, $^1J_{FC}$ = 272.4 Hz, CF_3), 125.01 (d, J_{PC} = 7.0 Hz, Aromatic C), 123.14 (br d, $^1J_{PC}$ = 110.5 Hz, *ipso*-Ph), 118.05 (sp, $^3J_{FC}$ = 3.9 Hz, *p*-BAr^F_4), 112.75 (br d, $^1J_{PC}$ = 74.1 Hz, 4,6-dbf), 28.41 (s, $CH(CH_3)_2$), 23.12 (s, $CH(CH_3)_2$); elemental analysis calcd (%) for $C_{78}H_{49}BF_{20}N_2OP_2$: C 61.96, H 3.69, N 1.68; found: C 62.00, H 3.58, N 1.83.

[L^2H^+][$B(C_6H_3(CF_3)_2)_4^-$] (**2a**). **2a** was prepared similarly to **1a** from $\mathbf{L^2}$ (200 mg, 0.268 mmol) and the oxonium acid $[H(OEt_2)_2^+][B(C_6H_3(CF_3)_2)_4^-]$ (271 mg, 268 mmol), yielding **2a** as a light yellow powder in 90.7% yield (392 mg, 0.243 mmol). ^{1}H NMR (CD_2Cl_2): δ 8.42 (d, 2H, $^3J_{HH}$ = 7.8 Hz, 1,9-dbf), 7.74 (s, 8H, *m*-BAr^F_4), 7.66–7.50 (ov m, 10H, 2,8-dbf + *p*-Ph + *p*-BAr^F_4), 7.48–7.28 (ov m, 18H, *o*-Ph + *m*-Ph + 3,7-dbf), 6.88 (d, 2H, $^3J_{HH}$ = 7.4 Hz, 4-*o*-Tol), 6.71 (t, 2H, $^3J_{HH}$ = 7.4 Hz, 3-*o*-Tol), 6.57 (t, 2H, $^3J_{HH}$ = 7.6 Hz, 2-*o*-Tol), 6.32 (d, 2H, $^3J_{HH}$ = 7.8 Hz, 1-*o*-Tol), 6.22 (s, 1H, NH), 1.84 (s, 6H, CH_3 *o*-Tol). The acidic NH proton was not observed. $^{31}P\{^1H\}$ NMR (CD_2Cl_2): δ 14.3; $^{19}F\{^1H\}$ NMR (CD_2Cl_2): δ −61.9; $^{11}B\{^1H\}$ NMR (CD_2Cl_2): δ −6.6. $^{13}C\{^1H\}$ NMR (CD_2Cl_2): δ 162.31 (q, $^1J_{BC}$ = 50.0 Hz, *ipso*-BAr^F_4), 158.10 (d, J_{CP} = 1.6 Hz, aromatic C), 141.22 (d, J_{CP} = 3.5 Hz, aromatic C), 135.61 (d, J_{CP} = 12.6 Hz, aromatic C), 135.35 (br s, *o*-BAr^F_4), 134.53 (d, $^4J_{PC}$ = 3.0 Hz, *p*-Ph), 133.19 (d, $^2J_{CP}$ = 10.4 Hz, *o*-Ph), 133.17 (d, $^3J_{PC}$ = 7.0 Hz, 3,7-dbf), 131.22 (s, 4-*o*-Tol), 129.94 (d, $^3J_{CP}$ = 13.1 Hz, *m*-Ph), 129.42 (qq, $^2J_{FC}$ = 31.5 Hz, $^3J_{BC}$ = 2.9 Hz, *m*-BAr^F_4), 127.86 (d, $^4J_{CP}$ = 2.5 Hz, 1,9-dbf), 127.12 (d, $^4J_{CP}$ = 1.7 Hz, 2-*o*-Tol), 125.35 (d, $^3J_{CP}$ = 6.2 Hz, 2,8-dbf), 125.24 (d, $^3J_{CP}$ = 2.2 Hz, 1-*o*-Tol), 125.14 (q, $^1J_{FC}$ = 272.4 Hz, CF_3), 124.96 (dd, J_{CP} = 6.0 Hz, J_{CP} = 0.9 Hz, aromatic C), 124.46 (d, $^1J_{CP}$ = 110.5 Hz, *ipso*-Ph), 124.10 (d, $^5J_{CP}$ = 1.9 Hz, 3-*o*-Tol), 118.04 (sp, $^3J_{CF}$ = 4.2 Hz, *p*-BAr^F_4), 112.94 (d, $^1J_{PC}$ = 86.7 Hz, 4,6-dbf), 18.87 (s, *o*-Tol CH_3); elemental analysis calcd (%) for $C_{82}H_{53}BF_{24}N_2OP_2$: C 61.13, H 3.32, N 1.74; found: C 61.03, H 3.02, N 1.85.

[L^3H^+][$B(C_6H_3(CF_3)_2)_4^-$] (**3a**). **3a** was prepared similarly to **1a** from $\mathbf{L^3}$ (0.200 g, 0.278 mmol) and the oxonium acid $[H(OEt_2)_2][B(C_6H_3(CF_3)_2)]$ (0.281 mg, 0.278 mmol), affording **3a** as a pale yellow powder in 89.2% yield (392 mg, 0.248 mmol). ^{1}H NMR (CD_2Cl_2): δ 8.41 (dt, 2H, $^3J_{HH}$ = 7.8 Hz, $^4J_{HH}$ = 1.4 Hz), 7.74 (br s, 8H, *o*-BAr^F_4), 7.69–7.58 (ov m, 6H, *p*-Ph + 2,8-dbf), 7.57–7.38 (ov m, 22H, *p*-BAr^F_4 + *o*-Ph + *m*-Ph + 3,7-dbf), 7.02–6.85 (ov m, 6H, *m*- + *p*-*N*-Ph), 6.65 (d, 4H, $^3J_{HH}$ = 8.2 Hz, *o*-*N*-Ph). The acidic NH proton was not observed. $^{31}P\{^1H\}$ NMR (CD_2Cl_2): δ 19.2 (br s); $^{19}F\{^1H\}$ NMR (CD_2Cl_2): δ −62.8 (s); $^{11}B\{^1H\}$ NMR (CD_2Cl_2): δ −6.6 (s); $^{13}C\{^1H\}$ NMR (CD_2Cl_2): δ 162.34 (q, $^1J_{CB}$ = 50.0 Hz, *ipso*-BAr^F_4), 157.54 (d, J_{CP} = 1.4 Hz, aromatic C), 142.26 (br s, aromatic C), 135.38 (br s, *o*-BAr^F_4), 135.13 (d, $^4J_{CP}$ = 2.8 Hz, *p*-Ph), 133.53 (d, $^2J_{CP}$ = 10.9 Hz, *o*-Ph), 133.40 (d, $^2J_{CP}$ = 8.7 Hz, 3,7-dbf), 130.27 (d, $^3J_{CP}$ = 13.3 Hz, *m*-Ph), 129.89 (s, *m*-*N*-Ph), 129.46 (qq, $^2J_{CF}$ = 31.5 Hz, $^3J_{CB}$ = 2.9 Hz, *m*-BAr^F_4), 128.34 (d, $^4J_{CP}$ = 2.6 Hz, 1,9-dbf), 125.74 (d, $^3J_{CP}$ = 11.3 Hz, 2,8-dbf), 125.17 (q, $^1J_{CF}$ = 272.4 Hz, CF_3), 125.09 (dd, J_{CP} = 6.4 Hz, J_{CP} = 1.0 Hz, aromatic C), 124.63 (d, $^3J_{CP}$ = 10.1 Hz, *o*-*N*-Ph), 123.71 (s, *p*-*N*-Ph), 123.56 (d, $^1J_{CP}$ = 106.9 Hz, *ipso*-Ph), 118.06 (br sp, $^3J_{CF}$ = 4.0 Hz, *p*-BAr^F_4), 110.87 (d, $^1J_{CP}$ = 96.2 Hz, 4,6-dbf); elemental analysis calcd (%) for $C_{80}H_{49}BF_{24}N_2OP_2$: C 60.70, H 3.12, N 1.77; found: C 60.54, H 2.95, N 1.76.

[L^1H^+][BPh_4^-] (**1b**). This synthesis was performed without exclusion of air and moisture. To a solution of $\mathbf{L^1}$ in (0.50 g, 0.62 mmol) in methanol (5 mL) one equiv of aqueous 1 M HCl (0.62 mL, 0.62 mmol) was added. To this solution a separately prepared solution of $NaBPh_4$ (0.23 g, 0.67 mmol) in methanol (2 mL) was added with rapid stirring, immediately generating a flocculent white precipitate. This precipitate was collected by filtration, washed with methanol (3 × 2 mL) and pentane (3 × 2 mL), and dried *in vacuo*, yielding the compound as a white powder in 63% yield (0.44 g, 0.39 mmol). ^{1}H NMR (acetone-d_6): δ 8.72 (d, 2H, $^3J_{HH}$ = 7.7 Hz, 1,9-dbf), 8.00 (dd, 2H, $^3J_{PH}$ = 13.6 Hz, $^3J_{HH}$ = 7.7 Hz, 3,7-dbf), 7.78 (t, 2H, $^3J_{HH}$ = 7.7 Hz, 2,8-dbf), 7.60–7.46 (ov m, 14H, *o*-Ph + *p*-Ph), 7.40–7.25 (ov m, 16H, *o*-BPh_4 + *m*-Ph), 7.14 (d, 2H, $^3J_{HH}$ = 7.5 Hz, 4-NAr), 6.91 (t, 8H, $^3J_{HH}$ = 7.4 Hz, *m*-BPh_4), 6.85 (t, 2H, $^3J_{HH}$ = 7.5 Hz, 3-NAr), 6.76 (t, 4H, $^3J_{HH}$ = 7.2 Hz, *p*-BPh_4), 6.63 (t, 2H, $^3J_{HH}$ = 7.5 Hz, 2-NAr), 6.48 (d, 2H, $^3J_{HH}$ = 7.9 Hz, 1-NAr), 4.72 (br s, 1H, N*H*), 3.50 (sp, 2H, $^3J_{HH}$ = 6.9 Hz, C*H*$(CH_3)_2$), 1.08 (d, 12H, $^3J_{HH}$ = 6.9 Hz, CH(C*H*$_3$)$_2$); $^{31}P\{^1H\}$ NMR (acetone-d_6): δ 13.7 (br s); $^{11}B\{^1H\}$ NMR (acetone-d_6): δ −6.5; $^{13}C\{^1H\}$ NMR (acetone-d_6): δ 165.00 (q, $^1J_{BC}$ = 49.4 Hz, *ipso*-BPh_4), 157.70 (d, J_{PC} = 2.8 Hz), 145.24 (d, J_{PC} = 11.7 Hz), 137.10

(q, $^2J_{BC}$ = 1.4 Hz, *o*-BPh_4), 135.06 (d, $^2J_{PC}$ = 6.8 Hz, 3,7-dbf), 134.80 (br s, *p*-Ph), 133.65 (d, $^2J_{PC}$ = 10.8 Hz, *o*-Ph), 130.29 (d, $^3J_{PC}$ = 13.1 Hz, *m*-Ph), 128.88 (br s, 1,9-dbf), 126.94 (d, $^4J_{PC}$ = 1.3 Hz, 2-NAr), 126.85 (br s, 4-NAr), 126.20 (br s, 2,8-dbf), 126.07 (q, $^3J_{BC}$ = 2.8 Hz, *m*-BPh_4), 125.84 (dd, J_{PC} = 6.8 Hz, J_{CP} = 1.1 Hz), 125.25 (br s, 1-NAr), 124.24 (br s, 3-NAr), 122.30 (s, *p*-BPh_4), 28.61 (s, $CH(CH_3)_2$), 23.41 (s, $CH(CH_3)_2$), 3 quaternary carbons are not observed; elemental analysis calcd (%) for $C_{78}H_{69}BN_2OP_2{\cdot}0.5CH_3OH$: C 82.77, H 6.28, N 2.46; found: C 82.91, H 6.07, N 2.47.

[L^2H^+][BPh_4^-] (2b). **2b** was prepared similarly to **1b** from L^2 (0.500 g, 0.670 mmol), 1 M HCl (0.67 mL, 0.67 mmol), and $NaBPh_4$ (0.25 g, 0.73 mmol), yielding **2b** as a white powder in 70.4% yield (0.504 g, 0.472 mmol). ^{1}H NMR (acetone-d_6): δ 8.70 (d, 2H, $^3J_{HH}$ = 7.7 Hz, 1,9-dbf), 7.90 (dd, 2H, $^3J_{PH}$ = 14.2 Hz, $^3J_{HH}$ = 7.7 Hz, 3,7-dbf), 7.72 (td, 2H, $^3J_{HH}$ = 7.7 Hz, $^4J_{PH}$ = 1.8 Hz, 2,8-dbf), 7.64–7.49 (ov m, 12H, *o*-Ph + *p*-Ph), 7.39–7.28 (ov m, 16H, *o*-BPh_4 + *m*-Ph), 7.02 (d, 2H, $^3J_{HH}$ = 7.3 Hz, 4-*o*-Tol), 6.91 (t, 8H, $^3J_{HH}$ = 7.3 Hz, *m*-BPh_4), 6.81–6.72 (ov m, 6H, *p*-BPh_4 + 3-*o*-Tol), 6.67 (t, 2H, $^3J_{HH}$ = 7.5 Hz, 2-*o*-Tol), 6.42 (d, 2H, $^3J_{HH}$ = 7.7 Hz, 1-*o*-Tol), 4.17 (br s, 1H, N*H*), 2.14 (s, 6H, CH_3 *o*-Tol); ^{31}P{^{1}H} NMR (acetone-d_6): δ 12.6 (br s); ^{11}B{^{1}H} NMR (acetone-d_6): δ −6.5; ^{13}C{^{1}H} NMR (acetone-d_6): δ 165.00 (q, $^1J_{BC}$ = 49.4 Hz, *ipso*-BPh_4), 157.78 (d, J_{CP} = 2.2 Hz), 142.18 (br s), 137.10 (q, $^2J_{BC}$ = 1.4 Hz, *o*-BPh_4), 135.21 (d, $^2J_{CP}$ = 7.6 Hz, 3,7-dbf), 134.60 (d, $^4J_{CP}$ = 2.1 Hz, *p*-Ph), 133.66 (d, $^2J_{CP}$ = 10.8 Hz, *o*-Ph), 131.39 (s, 4-*o*-Tol), 130.18 (d, $^3J_{CP}$ = 13.1 Hz, *m*-Ph), 128.61 (s, 1,9-dbf), 127.19 (d, $^4J_{CP}$ = 1.3 Hz, 2-*o*-Tol), 126.05 (q, $^3J_{CP}$ = 2.8 Hz, *m*-BPh_4), 125.88 (d, $^3J_{CP}$ = 10.6 Hz, 2,8-dbf), 125.80 (dd, J_{CP} = 6.6 Hz, J_{CP} = 1.1 Hz), 124.87 (br s, 1-*o*-Tol), 123.36 (br s, 3-*o*-Tol), 122.30 (s, *p*-BPh_4), 19.31 (s, CH_3 *o*-Tol), 3 quaternary carbons not observed; elemental analysis calcd (%) for $C_{74}H_{61}BN_2OP_2{\cdot}0.5CH_3OH$: C 82.62, H 5.86, N 2.59; found: C 82.72, H 6.30, N 2.41.

[L^3H^+][BPh_4^-] (3b). **3b** was prepared similarly to **1b** from L^3 (0.50 g, 0.70 mmol), 1 M HCl (0.70 mL, 0.70 mmol), and $NaBPh_4$ (0.24 g, 0.70 mmol), giving **3b** as a white powder in 76% yield (0.55 g, 0.53 mmol). ^{1}H NMR (acetone-d_6): δ 8.67 (d, 2H, $^3J_{HH}$ = 7.7 Hz, 1,9-dbf), 7.90 (dd, 2H, $^3J_{PH}$ = 14.2 Hz, $^3J_{HH}$ = 7.7 Hz, 3,7-dbf), 7.78–7.64 (ov m, 10H, *o*-Ph + 2,8-dbf), 7.59 (t, 4H, $^3J_{HH}$ = 7.1 Hz, *p*-Ph), 7.44 (td, 8H, $^3J_{HH}$ = 7.5 Hz, $^4J_{PH}$ = 3.5 Hz, *m*-Ph), 7.35 (m, 8H, *o*-BPh_4), 7.02 (t, 4H, $^3J_{HH}$ = 7.5 Hz, *m*-NPh), 6.91 (t, 8H, $^3J_{HH}$ = 7.3 Hz, *m*-BPh_4), 6.82 (t, 2H, $^3J_{HH}$ = 7.5 Hz, *p*-NPh), 6.80–6.70 (ov m, 8H, *p*-BPh_4 + *o*-NPh), 4.76 (br s, 1H, N*H*); ^{31}P{^{1}H} NMR (acetone-d_6): δ 14.5 (br s); ^{11}B{^{1}H} NMR (acetone-d_6): δ −6.5; ^{13}C{^{1}H} NMR (acetone-d_6): δ 165.00 (q, $^1J_{BC}$ = 49.4 Hz), 157.50 (d, J_{PC} = 2.4 Hz), 144.77 (s), 137.10 (q, J_{BC} = 1.4 Hz, *o*-BPh_4), 134.91 (d, J_{PC} = 3.0 Hz, *p*-Ph), 134.76 (d, J_{PC} = 7.8 Hz, 3,7-dbf), 133.86 (d, $^2J_{PC}$ = 11.0 Hz, *o*-Ph), 130.50 (d, $^3J_{PC}$ = 13.2 Hz, *m*-Ph), 129.90 (d, $^4J_{PC}$ = 0.5 Hz, *m*-NPh), 128.76 (d, $^4J_{PC}$ = 2.6 Hz, 1,9-dbf), 126.06 (q, $^3J_{BC}$ = 2.8 Hz, *m*-BPh_4), 125.89 (s, 2,8-dbf), 125.79 (dd, J_{PC} = 6.8 Hz, J_{PC} = 1.1 Hz), 125.06 (d, $^1J_{PC}$ = 105.6 Hz, *ipso*-Ph), 123.39 (d, $^3J_{PC}$ = 11.7 Hz, *o*-NPh), 122.31 (s, *p*-BPh_4), 122.06 (s), 111.22 (d, $^1J_{PC}$ = 97.8 Hz, 4,6-dbf); elemental analysis calcd (%) for $C_{72}H_{57}BN_2OP_2{\cdot}0.5CH_3OH$: C 82.54, H 5.64, N 2.66; found: C 82.69, H 5.50, N 2.54.

[$L^1ZnCH_3^+$][$B(C_6H_3(CF_3)_2)_4^-$] (4a). In a 20 mL vial, 200 mg (0.120 mmol) of **1a** was dissolved in 1 mL of CH_2Cl_2. To this yellow solution an excess of $ZnMe_2$ was added as a 1.2 M solution in toluene (150 μL, 0.180 mmol). The resulting reaction mixture was allowed to stand at ambient temperature for 90 min. The solvent was then removed *in vacuo*, giving the crude product as a red/orange oil. The oil was washed with pentane (3 × 1 mL) and dried *in vacuo*, affording **4a** as a light yellow powder in 96.7% yield (202 mg, 0.116 mmol). ^{1}H NMR (CD_2Cl_2): δ 8.51 (d, 2H, $^3J_{HH}$ = 7.8 Hz, 1,9-dbf), 7.74 (br s, 8H, *o*-BAr^F_4), 7.64 (t, 2H, $^3J_{HH}$ = 7.6 Hz, *p*-Ph), 7.60–7.43 (ov m, 12H, 2,8-dbf + *p*-BAr^F_4 + *p*-Ph + *o*-Ph), 7.38 (td, 4H, $^3J_{HH}$ = 7.6 Hz, $^4J_{PH}$ = 3.5 Hz, *m*-Ph), 7.27 (td, 4H, $^3J_{HH}$ = 7.6 Hz, $^4J_{PH}$ = 3.5 Hz, *m*-Ph), 6.99 (dd, 2H, $^3J_{PH}$ = 11.8 Hz, $^3J_{HH}$ = 7.5 Hz, 3,7-dbf), 6.92–6.75 (ov m, 8H, *o*-Ph + 3-NAr + 4-NAr), 6.43 (t, 2H, $^3J_{HH}$ = 7.9 Hz, 2-NAr), 6.30 (d, 2H, $^3J_{HH}$ = 7.9 Hz, 1-NAr), 3.23 (sp, 2H, $^3J_{HH}$ = 6.7 Hz, $CH(CH_3)_2$), 0.84 (d, 6H, $^3J_{HH}$ = 6.7 Hz, $CH(CH_3)_2$), 0.36 (d, 6H, $^3J_{HH}$ = 6.7 Hz, $CH(CH_3)_2$), −0.88 (s, 3H, $ZnCH_3$); ^{31}P{^{1}H} NMR (CD_2Cl_2): δ 22.7 (s); ^{19}F{^{1}H} NMR (CD_2Cl_2): δ −61.9 (s); ^{11}B{^{1}H} NMR (CD_2Cl_2): δ −6.6 (s); ^{13}C{^{1}H} NMR (CD_2Cl_2): δ 162.31 (q, $^1J_{BC}$ = 49.9 Hz, *ipso*-BAr^F_4), 158.43 (s, Aromatic C), 146.00 (d, J_{PC} = 9.2 Hz, Aromatic C), 140.99 (d, J_{PC} = 7.8 Hz, Aromatic C), 135.34 (br s, *o*-BAr^F_4), 135.03 (d, $^4J_{PC}$ = 2.8 Hz, *p*-Ph), 134.35 (d, $^2J_{PC}$ = 10.7 Hz, *o*-Ph), 134.19 (d, $^2J_{PC}$ = 4.8 Hz, 3,7-dbf), 134.13 (s, *p*-Ph), 133.65 (d, $^2J_{PC}$ = 9.1 Hz, *o*-Ph), 130.12 (d, $^3J_{PC}$ = 13.2 Hz, *m*-Ph), 129.42 (qq, $^2J_{FC}$ = 31.5 Hz, $^3J_{BC}$ = 2.9 Hz, *m*-BAr^F_4), 129.42 (d, $^3J_{PC}$ = 12.3 Hz, *m*-Ph), 128.06 (d, $^4J_{PC}$ = 2.4 Hz, 1,9-dbf), 127.57 (d, $^3J_{PC}$ = 6.0 Hz, 1-NAr), 127.27 (d, $^5J_{PC}$ = 2.6 Hz, 3-NAr), 126.79 (d, $^4J_{PC}$ = 3.2 Hz, 2-NAr), 125.63 (d, $^3J_{PC}$ = 10.4 Hz, 2,8-dbf), 125.46 (d, $^4J_{PC}$ = 3.4 Hz, 4-NAr), 125.13 (q, $^1J_{FC}$ = 272.5 Hz, CF_3), 124.64 (d, J_{PC} = 6.0 Hz, Aromatic C), 124.39 (d, $^1J_{PC}$ = 97.1 Hz, *ipso*-Ph), 123.74 (d, $^1J_{PC}$ = 117.6 Hz, *ipso*-Ph), 118.04 (br sp, $^3J_{FC}$ = 4.2 Hz, *p*-BAr^F_4), 114.15 (d, $^1J_{PC}$ = 90.3 Hz, 4,6-dbf), 27.90 (s, $CH(CH_3)_2$), 24.63 (s, $CH(CH_3)_2$), 23.19 (s, $CH(CH_3)_2$), −3.48 ($ZnCH_3$); Elemental analysis calcd (%) for $C_{87}H_{63}BF_{24}N_2OP_2Zn{\cdot}0.5CH_2Cl_2$: C 58.74, H 3.61, N 1.57; found: C 58.73, H 3.32, N 1.63.

[$L^2ZnCH_3^+$][$B(C_6H_3(CF_3)_2)_4^-$] (5a). Complex **5a** was prepared similarly to **4a** from **2a** (200 mg, 0.124 mmol) and dimethylzinc (150 μL of a 1.2 M solution in toluene, 180 mmol). After addition of $ZnMe_2$, the solution was triturated briefly and allowed to stand at ambient temperature for 2 h. The majority of the solvent was removed *in vacuo* giving a red/orange oil. Addition of 1 mL of pentane to this resulted in crystallization of the product. The pale yellow crystals were washed with pentane (3 x 1 mL) and dried *in vacuo*, affording **5a** in 96.8% yield (203 mg, 0.120 mmol). ^{1}H NMR (C_6D_5Br, 0 °C): δ 8.27 (s, 8H, *o*-BAr^F_4), 7.88 (d, 1H, $^3J_{HH}$ = 7.8 Hz, 1,9-dbf), 7.83 (d, 1H, $^3J_{HH}$ = 7.8 Hz, 1,9-dbf), 7.52 (s, 4H, *p*-BAr^F_4), 7.42 (dd, 2H, $^3J_{PH}$ = 12.4 Hz, $^3J_{HH}$ = 7.8 Hz, *p*-Ph), 7.36–7.24 (ov m, 2H, obscured by solvent, *p*-Ph), 7.24–7.06 (ov m, 6H, *o*-Ph + 2,8-dbf), 7.06–6.65

(ov m, 16H, *m*-Ph + *o*-Ph + 3,7-dbf + 3-*o*-Tol + 4-*o*-Tol), 6.65–6.56 (ov m, 2H, 3-NAr + 4-NAr), 6.37 (br s, 1H, 2-NAr), 6.25–6.11 (ov m, 2H, 2-*o*-Tol + 1-*o*-Tol), 5.86 (d, 1H, $^{3}J_{HH}$ = 7.8 Hz, 1-NAr), 1.79 (s, 3H, *o*-Tol CH_3), 1.55 (s, 3H, *o*-Tol CH_3), −0.35 (s, 1.5H, $ZnCH_3$), −0.88 (s, 1.5H, $ZnCH_3$); $^{31}P\{^{1}H\}$ NMR (C_6D_5Br, 0 °C): δ 24.1 (s), 21.7 (s); $^{31}P\{^{1}H\}$ NMR (C_6D_5Br, 100 °C): δ 23.4 (s); $^{19}F\{^{1}H\}$ NMR (C_6D_5Br, 25 °C): δ −61.5 (s); $^{11}B\{^{1}H\}$ NMR (C_6D_5Br, 25 °C): δ −5.8 (s); $^{13}C\{^{1}H\}$ NMR (C_6D_5Br, 0 °C): δ 162.37 (q, J_{BC} = 49.8 Hz, *ipso*-BAr^{F}_4), 158.07 (s), 157.62 (s), 142.82 (d, J_{PC} = 8.0 Hz), 140.86 (d, J_{PC} = 8.0 Hz), 136.39 (d, J_{PC} = 7.5 Hz), 135.26 (s), 135.07 (s), 134.36(s), 133.79 (d, J_{PC} = 6.5 Hz), 133.64 (s), 133.41 (d, J_{PC} = 10.3 Hz), 132.75 (d, J_{PC} = 9.6 Hz), 132.69 (d, J_{PC} = 10.1 Hz), 132.28 (d, J_{PC} = 9.6 Hz), 131.36 (s), 130.10 (s), 129.51 (d, J_{PC} = 13.3 Hz), 128.96 (d, J_{PC} = 8.9 Hz), 128.79 (d, J_{PC} = 8.7 Hz), 127.50 (d, J_{PC} = 10.9 Hz), 127.34 (br s), 126.83 (s), 126.32 (d, J_{PC} = 5.9 Hz), 125.80 (d, J_{PC} = 6.5 Hz), 124.96 (d, J_{PC} = 10.7 Hz), 124.76 (q, J_{FC} = 272.93 Hz, CF_3), 124.53 (d, J_{PC} = 10.4 Hz), 117.72 (br s), 112.94 (d, J_{PC} = 79.4 Hz), 111.74 (d, J_{PC} = 79.4 Hz), 19.31 (s), 18.08 (s), −3.42 (s), −6.77 (s). The resonances of several quaternary carbon atoms (6 total) are obscured by solvent or are too broad to be observed. Elemental analysis calcd (%) for $C_{83}H_{55}BF_{24}N_2OP_2Zn$: C 58.97, H 3.28, N 1.66; found: C 58.93, H 3.29, N 1.66.

[$L^3ZnCH_3^+$][$B(C_6H_3(CF_3)_2)_4^-$] (6a). Complex **6a** was prepared similarly to **4a** from **3a** (200 mg, 0.126 mmol) and excess dimethylzinc (1.2 M in toluene, 150 μL, 180 mmol), affording the product as a light yellow powder in 93.3% yield (196 mg, 118 mmol). ^{1}H NMR (CD_2Cl_2): δ 8.38 (d, 2H, $^{3}J_{HH}$ = 7.9 Hz, 1,9-dbf), 7.75 (br s, 8H, *o*-BAr^{F}_4), 7.70–7.50 (ov m, 18H, 2,8-dbf + *p*-Ph + *o*-Ph + *p*-BAr^{F}_4), 7.45 (dd, 8H, $^{3}J_{PH}$ = 7.6 Hz, $^{3}J_{HH}$ = 3.3 Hz, *m*-Ph), 7.31 (dd, 2H, $^{3}J_{PH}$ = 12.6 Hz, $^{3}J_{HH}$ = 7.7 Hz, 3,7-dbf), 6.87–6.69 (ov m, 6H, *m*-NPh + *p*-NPh), 6.58 (m, 4H, *o*-NPh), −1.02 (s, 3H, $ZnCH_3$); $^{31}P\{^{1}H\}$ NMR (CD_2Cl_2): δ 25.3 (s); $^{19}F\{^{1}H\}$ NMR (CD_2Cl_2): δ −61.9 (s); $^{11}B\{^{1}H\}$ NMR (CD_2Cl_2): δ −6.6 (s); $^{13}C\{^{1}H\}$ NMR (CD_2Cl_2): δ 162.31 (q, $^{1}J_{BC}$ = 49.8 Hz, *ipso*-BAr^{F}_4), 156.78 (s, Aromatic C), 145.57 (d, J_{PC} = 5.4 Hz, Aromatic C), 135.36 (br s, *o*-BAr^{F}_4), 134.53 (d, $^{3}J_{CP}$ = 3.0 Hz), 133.85 (d, $^{2}J_{PC}$ = 10.3 Hz, *o*-Ph), 132.61 (d, $^{4}J_{PC}$ = 8.2 Hz, 3,7-dbf), 129.95 (d, $^{3}J_{PC}$ = 12.7 Hz, *m*-Ph), 129.42 (qq, $^{2}J_{FC}$ = 31.5 Hz, $^{3}J_{BC}$ = 2.9 Hz, *m*-BAr^{F}_4), 129.71 (s, *m*-NPh), 127.89 (d, $^{4}J_{CP}$ = 2.6 Hz, 1,9-dbf), 126.20 (d, $^{4}J_{PC}$ = 11.6 Hz, *p*-Ph), 126.16 (d, $^{3}J_{CP}$ = 9.9 Hz, *o*-NPh), 125.13 (q, $^{1}J_{FC}$ = 272.4 Hz, CF_3), 124.96 (d, $^{1}J_{CP}$ = 99.1 Hz, *ipso*-Ph), 124.86 (d, J_{PC} = 6.3 Hz, Aromatic C), 123.54 (d, $^{5}J_{PC}$ = 2.6 Hz), 118.04 (sp, $^{3}J_{FC}$ = 4.0 Hz), 113.27 (d, $^{1}J_{PC}$ = 107.7 Hz, 4,6-dbf), −11.95 (s, $ZnCH_3$). Elemental analysis calcd (%) for $C_{81}H_{51}BF_{24}N_2OP_2Zn{\cdot}0.5CH_2Cl_2$: C 57.42, H 3.07, N 1.64; found: C 57.42, H 2.77, N 1.59.

[$L^1ZnCH_3^+$][BPh_4^-] (4b). To a solution of **1b** (200 mg, 0.178 mmol) in bromobenzene (1 mL), dimethylzinc was added as a 1.2 M solution in toluene (165 μL, 0.198 mmol). The resulting red solution was left to stand at ambient temperature for 30 min. To this 5 mL of pentane was added, causing precipitation of the product as a red oil. The supernatant was decanted, washed with pentane (2 × 1 mL), and dried *in vacuo*, giving the compound in quantitative yield (214 mg, 0.178 mmol). ^{1}H NMR (CD_2Cl_2): δ 8.51 (d, 2H, $^{3}J_{HH}$ = 7.9 Hz, 1,9-dbf), 7.70–7.42 (ov m, 14H, *o*-Ph + *p*-Ph + 2,8-dbf), 7.40–7.23 (ov m, 18H, *o*-BPh_4 + *m*-Ph + 3,7-dbf), 7.01 (t, 8H, $^{3}J_{HH}$ = 7.4 Hz, *m*-BPh_4), 6.91–6.75 (ov m, 8H, *p*-BPh_4 + 3-NAr + 4-NAr), 6.42 (t, 2H, $^{3}J_{HH}$ = 7.7 Hz, 2-NAr), 6.29 (d, 2H, $^{3}J_{HH}$ = 7.7 Hz, 1-NAr), 3.22 (sp, 2H, $^{3}J_{HH}$ = 6.8 Hz, $CH(CH_3)_2$), 0.84 (d, 6H, $^{3}J_{HH}$ = 6.8 Hz, $CH(CH_3)_2$), 0.36 (d, 6H, $^{3}J_{HH}$ = 6.8 Hz, $CH(CH_3)_2$), −0.90 (s, 3H, $ZnCH_3$); $^{31}P\{^{1}H\}$ NMR (CD_2Cl_2): δ 22.7 (s); $^{11}B\{^{1}H\}$ NMR (CD_2Cl_2): δ −6.6 (s); Material crystallized from CH_2Cl_2 was used for elemental analysis, and results were consistent with the retention of 0.5 equiv. of CH_2Cl_2. Elemental analysis calcd (%) for $C_{79}H_{71}BN_2OP_2Zn{\cdot}0.5CH_2Cl_2$: C 76.69, H 5.83, N 2.25; found: C 76.54, H 5.66, N 2.36.

[$L^2ZnCH_3^+$][BPh_4^-] (5b). Complex **5b** was prepared similarly to **4b** from **2b** (200 mg, 0.185 mmol) and dimethylzinc (1.2 M in toluene, 160 μL, 0.192 mmol) producing a white powder material, which was approximately 75% **5b** and 25% [L^2ZnPh^+][BPh_4^-], with an overall quantitative yield (212 mg, 185 mmol). Single crystals grown from this mixture were found to also contain an approximate 3 : 1 ratio of the methylzinc and phenylzinc products, respectively. Only the resonances of the primary product (**5b**) are listed below. ^{1}H NMR (CD_2Cl_2): δ 8.49 (d, 2H, $^{3}J_{HH}$ = 7.9 Hz, 1,9-dbf), 7.70–7.40 (br ov m, 14H, *o*-Ph + *p*-Ph + 2,8-dbf), 7.38–7.22 (br ov m, 16H, *m*-Ph + *o*-BPh_4), 7.12 (br s, 2H, 3,7-dbf), 7.00 (t, 8H, $^{3}J_{HH}$ = 7.5 Hz, *m*-BPh_4), 6.85 (t, 4H, $^{3}J_{HH}$ = 7.5 Hz, *p*-BPh_4), 6.77 (br ov m, 4H, 3-*o*-Tol + 4-*o*-Tol), 6.39 (br s, 2H, 2-*o*-Tol), 6.14 (br s, 1H, 1-*o*-Tol), 5.95 (br s, 1H, 1-*o*-Tol), 1.78 (br s, 3H, *o*-Tol CH_3), 1.61 (br s, 3H, *o*-Tol CH_3), −0.60 (br s, 1.5H, $ZnCH_3$), −0.93 (br s, 1.5H, $ZnCH_3$); $^{31}P\{^{1}H\}$ NMR (CD_2Cl_2): δ 22.2 (br s), 23.9 (br s); $^{11}B\{^{1}H\}$ NMR (CD_2Cl_2): δ −6.6 (s).

[$L^3ZnCH_3^+$][BPh_4^-] (6b). Complex **6b** was prepared similarly to **4b** from **3b** (200 mg, 192 mmol) and dimethylzinc (1.2 M in toluene, 165 μL, 198 mmol), yielding a 4 to 1 mixture of **4b** and a compound of the formula [L^3ZnPh^+][BPh_4^-] in a combined yield of 96.1% (207 mg, 185 mmol). Only the resonances of **6b** are listed below. ^{1}H NMR (CD_2Cl_2): δ 8.36 (d, 2H, $^{3}J_{HH}$ = 7.9 Hz, 1,9-dbf), 7.73–7.48 (ov m, 14H, *o*-Ph + *p*-Ph + 2,8-dbf), 7.44 (td, 8H, $^{3}J_{HH}$ = 7.7 Hz, $^{4}J_{PH}$ = 3.4 Hz, *m*-Ph), 7.35–7.20 (ov m, 10H, *o*-BPh_4 + 3,7-dbf), 7.00 (t, 8H, $^{3}J_{HH}$ = 7.5 Hz, *m*-BPh_4), 6.84 (t, 4H, $^{3}J_{HH}$ = 7.5, *p*-BPh_4), 6.80–6.69 (ov m, 6H, *m*-NPh + *p*-NPh), 6.57 (d, 4H, $^{3}J_{HH}$ = 7.2 Hz, *o*-NPh), −1.04 (s, 3H, $ZnCH_3$); $^{31}P\{^{1}H\}$ NMR (CD_2Cl_2): δ 25.3 (s); $^{11}B\{^{1}H\}$ NMR (CD_2Cl_2): δ −6.6 (s).

[$L^2ZnOCH(Me)CO_2Me^+$][$B(C_6H_3(CF_3)_2)_4^-$] (7). Stoichiometric amounts of **2a** (200 mg, 0.124 mmol) and ethylzinc lactate (24.5 mg, 0.124 mmol) were combined in a glass bomb with 3 mL of bromobenzene. The bomb was sealed and the yellow solution was heated, with stirring, to 100 °C for 2 h. The solution was then allowed to cool to ambient temperature and was filtered through celite into a glass vial. To this light yellow solution 1 mL of benzene and 10 mL of pentane were

added, resulting in a cloudy solution. After letting stand at ambient temperature for 18 h, the compound crystallized as a white microcrystalline material. The supernatant was decanted, the crystals were washed with pentane (3 × 1 mL) and dried *in vacuo*, giving 118 mg of the product. The supernatant was placed in a freezer at −35 °C, and after 6 days an additional crop of 50 mg of **7** was obtained, giving an overall yield of 76.2% (168 mg, 0.0945 mmol). ^{1}H NMR (C_6D_5Br, 80 °C): δ 8.11 (s, 8H, *o*-BAr^F_4), 7.99 (d, 2H, $^{3}J_{HH}$ = 7.8 Hz, 1,9-dbf), 7.57 (s, 4H, *p*-BAr^F_4), 7.40–7.13 (br ov m, 14H, *o*-Ph + *p*-Ph + 2,8-dbf), 7.12–6.88 (br ov m, 10H, *m*-Ph + 3,7-dbf), 6.73–6.63 (ov m, 4H, 3-*o*-Tol + 4-*o*-Tol), 6.57–6.38 (br ov m, 4H, 1-*o*-Tol + 2-*o*-Tol), 4.39 (q, 1H, $^{3}J_{HH}$ = 6.8 Hz, OC*H*MeCO$_2$Me), 2.89 (s, 3H, OCHMeCO$_2$*Me*), 1.56 (s, 3H, *o*-Tol CH$_3$), 1.35 (d, 3H, $^{3}J_{HH}$ = 6.8 Hz, OCH*Me*CO$_2$Me). Additionally, a small amount of a second isomer of the compound is evident, only in unique resonances of methyllactate CH and OCH$_3$ groups. These appear at δ 4.07 and 3.64, respectively, and are too weak to be observed in the ^{13}C NMR spectrum. ^{31}P{^{1}H} NMR (C_6D_5Br, 80 °C): δ 27.2 (s); ^{19}F{^{1}H} NMR (C_6D_5Br): δ −61.5 (s); ^{11}B{^{1}H} NMR (C_6D_5Br): δ −5.8 (s); ^{13}C{^{1}H} NMR (C_6D_5Br, 80 °C): δ 190.56 (s, OCHMe-*C*O$_2$Me), 162.24 (q, $^{1}J_{BC}$ = 50.0 Hz, *ipso*-BAr^F_4), 158.11 (s, Aromatic c), 142.93 (d, J_{CP} = 9.1 Hz, Aromatic C), 137.16 (d, J_{CP} = 7.1 Hz, Aromatic C), 135.10 (s, *o*-BAr^F_4), 133.79 (br s, *o*-Ph), 133.61 (d, $^{2}J_{CP}$ = 6.5 Hz, 3,7-dbf), 133.27 (br s, Aromatic C), 132.40 (d, $^{4}J_{CP}$ = 10.4 Hz, *p*-Ph), 130.54 (s, 3-*o*-Tol), 129.04 (br m, *m*-Ph), 128.50 (d, $^{3}J_{CP}$ = 5.7 Hz, 1-*o*-Tol), 127.02 (s, 1,9-dbf), 126.54 (s, 2-*o*-Tol), 125.00 (d, $^{4}J_{CP}$ = 3.5 Hz, 4-*o*-Tol), 124.80 (q, $^{1}J_{CF}$ = 273 Hz, CF_3), 124.32 (d, $^{3}J_{CP}$ = 10.7 Hz, 2,8-dbf), 117.62 (s, *p*-BAr^F_4), 113.08 (d, $^{1}J_{CP}$ = 92.7 Hz, 4,6-dbf), 70.92 (s, O*C*HMe-CO$_2$Me), 53.25 (s, OCHMeCO$_2$*Me*), 23.35 (s, OCH*Me*-CO$_2$Me), 17.91 (s, CH$_3$ *o*-Tol). Signals for *ipso*-Ph and *m*-BAr^F_4 were not observed. Elemental analysis calcd (%) for $C_{86}H_{59}BF_{24}N_2O_4P_2Zn$: C 58.08, H 3.34, N 1.58; found: C 58.20, H 3.00, N 1.59.

[L^{3}ZnOCH(Me)CO$_2$Me$^+$][B(C$_6$H$_3$(CF$_3$)$_2$)$_4^-$] (8). A stoichiometric amount of **3a** (100 mg, 0.063 mmol) and ethyl zinc lactate (12.5 mg, 0.063 mmol) were combined in a glass bomb with 5 mL of bromobenzene. The bomb was sealed and heated to 100 °C for two hours while stirring. The resulting red/orange solution was cooled to ambient temperature, and then filtered through celite into a glass vial. The volume was reduced under vacuum to ~3 mL and then 10 mL of pentane was added to precipitate the product. The resulting cloudy solution was placed in a freezer at −35 °C for 24 h. During this time, the product precipitated as a red/orange oil. The supernatant was decanted and the oil was washed with pentane (3 × 1 mL) and dried *in vacuo*, giving 62 mg of the compound as a light red/orange powder. The supernatant was returned to −35 °C for three more days, and an additional 18 mg of product was obtained, for an overall yield of 72% (80 mg, 0.046 mmol). Two distinct structural isomers are apparent in the ^{1}H and ^{13}C NMR spectra. ^{1}H NMR (CD_2Cl_2): δ 8.47 (dt, 1H, $^{3}J_{HH}$ = 7.8 Hz, $^{4}J_{HH}$ = 1.4 Hz, 1,9-dbf), 8.43 (dt, 1H, $^{3}J_{HH}$ = 7.8 Hz, $^{4}J_{HH}$ = 1.4 Hz, 1,9-dbf), 7.77 (br s, 8H, *m*-BAr^F_4), 7.72–7.40 (ov m, 28H, *o*-Ph + *m*-Ph + *p*-Ph + *p*-BAr^F_4 + 2,8-dbf + 3,7-dbf), 7.00 (t, 2H, $^{3}J_{HH}$ = 7.8 Hz, *p*-NPh), 6.92–6.84 (ov m, 4H, *m*-NPh), 6.69 (d, 2H, $^{3}J_{HH}$ = 7.8 Hz, *o*-NPh), 6.57 (m, 4H, *o*-NPh), 4.06 (q, 0.5 H, $^{3}J_{HH}$ = 6.8 Hz, OC*H*MeCO$_2$Me), 3.93 (s, 1.5H, OCHMe-CO$_2$*Me*), 3.44 (q, 0.5 H, $^{3}J_{HH}$ = 6.8 Hz, OC*H*MeCO$_2$Me), 3.42 (s, 1.5H, OCHMeCO$_2$*Me*), 1.36 (d, 1.5H, $^{3}J_{HH}$ = 6.8 Hz, OCH*Me*CO$_2$ Me), 0.87 (d, 1.5H, $^{3}J_{HH}$ = 6.8 Hz, OCH*Me*-CO$_2$Me); ^{31}P{^{1}H} NMR (CD_2Cl_2): δ 29.3 (s); ^{19}F{^{1}H}NMR (CD_2Cl_2): δ −61.9 (s); ^{11}B{^{1}H} NMR (CD_2Cl_2): δ −6.6 (s); ^{13}C{^{1}H} NMR (CD_2Cl_2): δ 191.4 (s, OCHMe*C*O$_2$Me), 185.48 (s, OCHMe*C*O$_2$Me), 162.31 (q, $^{1}J_{CB}$ = 49.9 Hz, *ipso*-BAr^F_4), 157.97 (s, Aromatic C), 145.20 (d, J_{CP} = 6.6 Hz, Aromatic C), 135.36 (br s, *o*-BAr^F_4), 134.61 (d, $^{4}J_{PC}$ = 3.0 Hz, *p*-Ph), 134.28 (d, $^{2}J_{PC}$ = 10.0 Hz, *o*-Ph), 134.27 (d, $^{4}J_{PC}$ = 3.0 Hz, *p*-Ph), 134.09 (d, $^{4}J_{PC}$ = 3.0 Hz, *p*-Ph), 133.82 (d, $^{2}J_{PC}$ = 10.1 Hz, *o*-Ph), 133.51 (d, $^{2}J_{PC}$ = 8.4 Hz, 3,7-dbf), 133.43 (d, $^{2}J_{PC}$ = 10.7 Hz, *o*-Ph), 133.16 (d, $^{2}J_{PC}$ = 8.0 Hz, 3,7-dbf), 131.36 (d, $^{1}J_{PC}$ = 101.4 Hz, *ipso*-Ph), 130.04 (d, $^{3}J_{PC}$ = 13.1 Hz, *m*-Ph), 129.70 (s, *p*-NPh), 129.60 (d, $^{2}J_{PC}$ = 12.7 Hz, *m*-Ph), 129.43 (qq, $^{2}J_{CF}$ = 31.3 Hz, $^{3}J_{CB}$ = 2.8 Hz, *m*-BAr^F_4), 129.23 (d, $^{4}J_{PC}$ = 2.8 Hz, *m*-NPh), 129.01 (d, $^{3}J_{PC}$ = 7.5 Hz, *o*-NPh), 127.80 (d, $^{4}J_{PC}$ = 2.3 Hz, 1,9-dbf), 127.55 (s, Aromatic C), 127.54 (d, $^{4}J_{PC}$ = 2.6 Hz, 1,9-dbf), 125.51 (d, $^{3}J_{PC}$ = 3.3 Hz, 2,8-dbf), 125.37 (d, $^{3}J_{PC}$ = 3.6 Hz, 2,8-dbf), 125.14 (q, $^{1}J_{CF}$ = 272.4 Hz, CF_3), 124.94 (d, $^{3}J_{PC}$ = 11.3 Hz, *o*-NPh), 124.45 (d, $^{4}J_{PC}$ = 3.6 Hz, *m*-NPh), 118.04 (sp, $^{3}J_{CF}$ = 4.1 Hz, *p*-BAr^F_4), 111.72 (d, $^{1}J_{PC}$ = 106.1 Hz, 4,6-dbf), 69.80 (s, O*C*HMeCO$_2$Me), 67.79 (s, O*C*HMeCO$_2$Me), 54.69 (s, OCHMeCO$_2$*Me*), 54.23 (s, OCHMeCO$_2$*Me*), 24.12 (s, OCH*Me*CO$_2$Me), 13.47 (s, OCH*Me*CO$_2$Me). (The ^{13}C spectrum contains 3 unique resonances for both the *o*-Ph and *p*-Ph atoms. The quaternary carbons, with the exception of the lactate moiety, are not split into two sets of resonances.) Elemental analysis calcd (%) for $C_{84}H_{55}BF_{24}N_2O_4P_2Zn$: C 57.64, H 3.17, N 1.60; found: C 57.77, H 2.85, N 2.03.

4.4 X-Ray structure determination

Crystals were grown from a concentrated CH_2Cl_2 solution of the compound at −35 °C for **L^1**, by slow diffusion of pentane into a benzene solution at 25 °C for **L^2** and **L^3**, by slow diffusion of benzene into a benzene/bromobenzene solution at 25 °C for **4b**, **5b**/**c** and **6b**/**c**, from a concentrated bromobenzene solution spiked with a small amount of benzene at −35 °C for **8**, and by slow diffusion of pentane into a CH_2Cl_2 solution of the compound at 25 °C for **7**. X-ray intensities were measured on a Bruker SMART APEX II (Mo-Kα radiation; λ = 0.71073 Å) instrument at a temperature of 173(2) K. Unit cell parameters were determined and refined on all reflections and data were integrated with APEX2 software.[31] Data reduction and correction for Lorentz polarization were performed using Saint-plus,[32] and scaling and absorption correction were performed using the SADABS software package.[33] Structure solution by direct methods and least-squares refinement on F^2 were performed using the SHELXTL software suite.[34] Non-hydrogen atoms were refined with anisotropic displacement parameters, while hydrogen atoms were placed in calculated positions and refined with a riding model. The SQUEEZE subroutine of the PLATON software package[35] was used to

model disordered solvent molecules in $\mathbf{L^2}$ and **6b**, and these solvent molecules are included in the respective formulae. Multi-scan absorption correction was employed in all cases. Structural figures were generated with ORTEP-3.[36]

Compound 4b. $C_{79}H_{71}BN_2OP_2Zn{\cdot}C_6H_6$, M = 1280.61, 0.60 × 0.50× × 0.19 mm^3, triclinic, $P\bar{1}$ (no. 2), a = 14.3702(7), b = 15.2542(7), c = 17.2588(8) Å, α = 81.451(1)°, β = 66.469(1)°, γ = 76.867(1)°, V = 3370.8(3) Å^3, ρ_c = 1.262 Mg m^{-3}, θ_{max} = 25.03°, 32 672 reflections measured, 11 879 independent [R_{int} = 0.0203], 10 320 with $I > 2\sigma(I)$, μ = 0.462 mm^{-1}, T_{max} = 0.9157, T_{min} = 0.7684, 834 parameters were refined, $R1/wR2$ [$I > 2\sigma(I)$]: 0.0302/0.0785, $R1/wR2$ (all refl.): 0.0370/0.0825, residual electron density between −0.287 and 0.337 eÅ^{-3}.

Compound 5b/5c. $C_{76.18}H_{63.47}BN_2OP_2Zn$, M = 1160.98, 0.42 × 0.21 × 0.04 mm^3, triclinic, $P\bar{1}$ (no. 2), a = 9.9214(8), b = 17.118(1), c = 18.475(1) Å, α = 86.754(1)°, β = 78.725(1)°, γ = 80.859(1)°, V = 3036.9(4) Å^3, ρ_c = 1.270 Mg m^{-3}, θ_{max} = 25.03°, 36 687 reflections measured, 10 686 independent [R_{int} = 0.0643], 6972 with $I > 2\sigma(I)$, μ = 0.505 mm^{-1}, T_{max} = 0.7456, T_{min} = 0.6780, 784 parameters were refined, $R1/wR2$ [$I > 2\sigma(I)$]: 0.0445/0.0849, $R1/wR2$ (all refl.): 0.0878/0.0987, residual electron density between −0.327 and 0.338 eÅ^{-3}.

Compound 6b/6c. $C_{74.65}H_{57.86}BN_2OP_2Zn{\cdot}C_6H_6{\cdot}C_6H_5Br$, M = 1372.16, 0.45 × 0.38 × 0.21 mm^3, triclinic, $P\bar{1}$ (no. 2), a = 9.9023(5), b = 16.8670(9), c = 20.711(1) Å, α = 101.974(1)°, β = 91.114(1)°, γ = 95.296(1)°, V = 3366.9(3) Å^3, ρ_c = 1.199 Mg m^{-3}, θ_{max} = 25.03°, 40 833 reflections measured, 11 870 independent [R_{int} = 0.0212], 10 042 with $I > 2\sigma(I)$, μ = 0.459 mm^{-1}, T_{max} = 0.7456, T_{min} = 0.6873, 829 parameters were refined, $R1/wR2$ [$I > 2\sigma(I)$]: 0.0387/0.1026, $R1/wR2$ (all refl.): 0.0465/0.1073, residual electron density between −0.421 and 0.684 eÅ^{-3}.

Compound 7. $C_{86}H_{59}BF_{24}N_2O_2P_2Zn{\cdot}0.83CH_2Cl_2$, M = 1848.96, 0.35 × 0.07 × 0.05 mm^3, triclinic, $P\bar{1}$ (no. 2), a = 11.466(1), b = 19.564(3), c = 19.662(3) Å, α = 99.640(2)°, β = 103.416(2)°, γ = 92.916(2)°, V = 4210(1) Å^3, ρ_c = 1.458 Mg m^{-3}, θ_{max} = 25.12°, 41 317 reflections measured, 14 955 independent [R_{int} = 0.1034], 7374 with $I > 2\sigma(I)$, μ = 0.487 mm^{-1}, T_{max} = 0.9770, T_{min} = 0.8476, 1170 parameters were refined, $R1/wR2$ [$I > 2\sigma(I)$]: 0.0785/0.1742, $R1/wR2$ (all refl.): 0.1704/0.2148, residual electron density between −0.665 and 0.724 eÅ^{-3}.

Compound 8. $C_{84}H_{55}BF_{24}N_2O_4P_2Zn{\cdot}C_6H_5Br_{0.38}$, M = 1857.89, 0.47 × 0.35 × 0.28 mm^3, monoclinic, $P2_1/c$ (no. 14), a = 18.781(1), b = 27.118(2), c = 18.651(1) Å, β = 116.785(1)°, V = 8479.6(9) Å^3, ρ_c = 1.455 Mg m^{-3}, θ_{max} = 25.03°, 101 702 reflections measured, 14 960 independent [R_{int} = 0.0443], 11 787 with $I > 2\sigma(I)$, μ = 0.612 mm^{-1}, T_{max} = 0.8489, T_{min} = 0.7608, 1339 parameters were refined, $R1/wR2$ [$I > 2\sigma(I)$]: 0.0613/0.1516, $R1/wR2$ (all refl.): 0.0797/0.1617, residual electron density between −0.636 and 0.852 eÅ^{-3}.

Acknowledgements

P.G.H. thanks NSERC, Canada Foundation for Innovation (CFI), Canada School of Energy and Environment and GreenCentre Canada for financial support. C.A.W. acknowledges NSERC and the Alberta Ingenuity Fund (Alberta Innovates) for student awards. Thanks also to Yun Yang of GreenCentre Canada for GPC measurements and Tony Montina (University of Lethbridge) for expert technical assistance.

Notes and references

1 See for example: (*a*) W. Piers and D. Emslie, *Coord. Chem. Rev.*, 2002, **233**, 131–155; (*b*) T. Hanusa, *Coord. Chem. Rev.*, 2000, **210**, 329–367; (*c*) V. Gibson and S. Spitzmesser, *Chem. Rev.*, 2003, **103**, 283–315.

2 See for example: (*a*) D. Benito-Garagorri and K. Kirchner, *Acc. Chem. Res.*, 2008, **41**, 201–213; (*b*) J. L. Bolliger, O. Blacque and C. M. Frech, *Angew. Chem. Int. Ed.*, 2007, **46**, 6514–6517; (*c*) A. Moncada, S. Manne, J. Tanski and L. Slaughter, *Organometallics*, 2006, **25**, 491–505; (*d*) E. Peris and R. Crabtree, *Coord. Chem. Rev.*, 2004, **248**, 2239–2246; (*e*) S. Gründemann, M. Albrecht, J. Loch, J. Faller and R. Crabtree, *Organometallics*, 2001, **20**, 5485–5488.

3 For selected reviews see: (*a*) V. C. Gibson and S. K. Spitzmesser, *Chem. Rev.*, 2003, **103**, 283–315; (*b*) G. W. Coates, *Chem. Rev.*, 2000, **100**, 1223–1252; (*c*) S. D. Ittel, L. K. Johnson and M. Brookhart, *Chem. Rev.*, 2000, **100**, 1169–1203; (*d*) H. H. Brintzinger, D. Fischer, R. Mulhaupt, B. Rieger and R. M. Waymouth, *Angew. Chem., Int. Ed.*, 1995, **34**, 1143–1170.

4 For selected reviews see: (*a*) K. Sudesh and T. Iwata, *Clean: Soil Air Water*, 2008, **36**, 433–442; (*b*) R. Auras, B. Harte and S. Selke, *Macromol. Biosci.*, 2004, **4**, 835–864; (*c*) J. Bogaert and P. Coszach, *Macromol. Symp.*, 2000, **153**, 287–303; (*d*) R. Drumright, P. Gruber and D. Henton, *Adv. Mater.*, 2000, **12**, 1841–1846.

5 (*a*) J. Dijkstra, H. Du and J. Feijen, *J. Polym. Chem.*, 2011, **2**, 520–527; (*b*) N. Ajellal, J.-F. Carpentier, C. Guillaume, S. M. Guillaume, M. Helou, V. Poirier, Y. Sarazin and A. Trifonov, *Dalton Trans.*, 2010, **39**, 8363–8376; (*c*) C. A. Wheaton, P. G. Hayes and B. J. Ireland, *Dalton Trans.*, 2009, 4832–4846; (*d*) R. H. Platel, L. M. Hodgson and C. K. Williams, *Polym. Rev.*, 2008, **48**, 11–63; (*e*) J. Wu, T.-L. Yu, C.-T. Chen and C.-C. Lin, *Coord. Chem. Rev.*, 2006, **250**, 602–626; (*f*) O. Dechy-Cabaret, B. Martin-Vaca and D. Bourissou, *Chem. Rev.*, 2004, **104**, 6147–6176.

6 Zinc complexes: See for example: (*a*) D. J. Darensbourg and O. Karroonnirun, *Inorg. Chem.*, 2010, **49**, 2360–2371; (*b*) F. Drouin, P. O. Oguadinma, T. J. J. Whitehorn, R. E. Prud'homme and F. Schaper, *Organometallics*, 2010, **29**, 2139–2147; (*c*) H.-Y. Chen, H.-Y. Tang and C.-C. Lin, *Macromolecules*, 2006, **39**, 3745–3752; (*d*) C. K. Williams, N. R. Brooks, M. A. Hillmyer and W. B. Tolman, *Chem. Commun.*, 2002, 2132–2133; (*e*) L. R. Rieth, D. R. Moore, E. B. Lobkovsky and G. W. Coates, *J. Am. Chem. Soc.*, 2002, **124**, 15239–15248; (*f*) M. H. Chisholm, J. C. Huffman and K. Phomphrai, *J. Chem. Soc., Dalton Trans.*, 2001, **2**, 333–224.

7 Magnesium complexes: See for example: (*a*) F. Drouin, T. J. J. Whitehorn and F. Schaper, *Dalton Trans.*, 2011, **40**, 1396–1400; (*b*) L. F. Sánchez-Barba, A. Garcés, J. Fernández-Baeza, A. Otero, C. Alonso-Moreno, A. Lara-Sánchez and A. M. Rodríguez , *Organometallics*, 2011, **30**, 2775–2789; (*c*) J. Ejfler, K. Krauzy-Dziedzic, S. Szafert, L. B. Jerzykiewicz and P. Sobota, *Eur. J. Inorg. Chem.*, 2010, 3602–3609; (*d*) M.-Y. Shen, Y.-L. Peng, W.-C. Hung and C.-C. Lin, *Dalton Trans.*, 2009, 9906–9913; (*e*) J. Ejfler, M. Kobylka, L. B. Jerzykiewicz and P. Sobota, *Dalton Trans.*, 2005, 2047–2050; (*f*) B. M. Chamberlain, M. Cheng, D. R. Moore, T. M. Ovitt, E. B. Lobkovsky and G. W. Coates, *J. Am. Chem. Soc.*, 2001, **123**, 3229–3238.

8 Calcium complexes: (*a*) See for example: H.-Y. Chen, H.-Y. Tang and C.-C. Lin, *Polymer*, 2007, **48**, 2257–2262; (*b*) M. H. Chisholm, J. C. Gallucci and K. Phomphrai, *Inorg. Chem.*, 2004, **43**, 6717–6725; (*c*) M. H. Chisholm, J. Gallucci and K. Phomphrai, *Chem.*

Commun., 2003, 48–49; (*d*) Z. Zhong, P. J. Dijkstra, C. Birg, M. Westerhausen and J. Feijen, *Macromolecules*, 2001, **34**, 3863–3868.
9 Aluminium complexes: See for example: (*a*) A. Otero, A. Lara-Sánchez, J. Fernández-Baeza, C. Alonso-Moreno, J. A. Castro-Osma, I. Márquez-Segovia, L. F. Sánchez-Barba, A. M. Rodríguez and J. C. Garcia-Martinez, *Organometallics*, 2011, **30**, 1507–1522; (*b*) A. D. Schwarz, Z. Chu and P. Mountford, *Organometallics*, 2010, **29**, 1246–1260; (*c*) D. J. Darensbourg and O. Karroonnirun, *Organometallics*, 2010, **29**, 5627–5634; (*d*) H. Du, A. H. Velders, P. J. Dijkstra, Z. Zhong, X. Chen and J. Feijen, *Macromolecules*, 2009, **42**, 1058–1066; (*e*) X. Pang, H. Du, X. Chen, X. Wang and X. Jing, *Chem. Eur. J*., 2008, **14**, 3126–3136; (*f*) H. Ma, G. Melillo, L. Oliva, T. P. Spaniol, U. Englert and J. Okuda, *Dalton Trans*., 2005, 721–727; (*g*) M. H. Chisholm, N. J. Patmore and Z. Zhou, *Chem. Commun*., 2005, 127–129.
10 Ga and In Complexes: See for example: (*a*) M. P. Blake, A. D. Schwarz and P. Mountford, *Organometallics*, 2011, **30**, 1202–1214; (*b*) P. Horeglad, P. Kruk and J. Pécaut, *Organometallics*, 2010, **29**, 3729–3734; (*c*) A. Pietrangelo, S. C. Knight, A. K. Gupta, L. J. Yao, M. A. Hillmyer and W. B. Tolman, *J. Am. Chem. Soc*., 2010, **132**, 11649–11657; (*d*) J.-C. Buffet, J. Okuda and P. L. Arnold, *Inorg. Chem*., 2010, **49**, 419–426; (*e*) A. F. Douglas, B. O. Patrick and P. Mehrkhodavandi, *Angew. Chem. Int. Ed*., 2008, **47**, 2290–2293.
11 Rare earth Complexes: See for example: (*a*) A. Buchard, R. H. Platel, A. Auffrant, X. F. Le Goff, P. Le Floch and C. K. Williams, *Organometallics*, 2010, **29**, 2892–2900; (*b*) H. E. Dyer, S. Huijser, N. Susperregui, F. Bonnet, A. D. Schwarz, R. Duchateau, L. Maron and P. Mountford, *Organometallics*, 2010, **29**, 3602–3621; (*c*) H. Ma, T. P. Spaniol and J. Okuda, *Inorg. Chem*., 2008, **47**, 3328–3339; (*d*) N. Barros, P. Mountford, S. M. Guillaume and L. Maron, *Chem. Eur. J*., 2008, **14**, 5507–5518; (*e*) X. Liu, X. Shang, T. Tang, N. Hu, F. Pei, D. Cui, X. Chen and X. Jing, *Organometallics*, 2007, **26**, 2747–2757; (*f*) A. Amgoune, C. M. Thomas and J.-F. Carpentier, *Pure Appl. Chem*., 2007, **79**, 2013–2030; (*g*) A. Amgoune, C. M. Thomas, T. Roisnel and J.-F. Carpentier, *Chem. Eur. J*., 2006, **12**, 169–179; (*h*) H. Ma, T. P. Spaniol and J. Okuda, *Angew. Chem. Int. Ed*., 2006, **45**, 7818–7821.
12 (*a*) M. Reinmuth, U. Wild, D. Rudolf, E. Kaifer, M. Enders, H. Wadepohl and H.-J. Himmel, *Eur. J. Inorg. Chem*., 2009, 4795–4808; (*b*) M. D. Hannant, M. Schormann and M. Bochmann, *J. Chem. Soc., Dalton Trans*., 2002, 4071–4073; (*c*) Y. Sarazin, M. Schormann and M. Bochmann, *Organometallics*, 2004, **23**, 3296–3302; (*d*) S. Dagorne, M. Bouyahyi, J. Vergnaud and J.-F. Carpentier, *Organometallics*, 2010, **29**, 1865–1868; (*e*) S. Dagorne, S. Bellemin-Laponnaz and R. Welter, *Organometallics*, 2004, **23**, 3053–3061.
13 (*a*) Y. Sarazin, B. Liu, T. Roisnel, L. Maron and J.-F. Carpentier, *J. Am. Chem. Soc*., 2011, **133**, 9069–9087; (*b*) M. G. Cushion and P. Mountford, *Chem. Commun*., 2011, **47**, 2276–2278; (*c*) Y. Sarazin, V. Poirier, T. Roisnel and J.-F. Carpentier, *Eur. J. Inorg. Chem*., 2010, 3423–3428; (*d*) J. Boerner, S. Herres-Pawlis, U. Floeke and K. Huber, *Eur. J. Inorg. Chem*., 2007, 5645–5651; (*e*) S. Dagorne, F. Le Bideau, R. Welter, S. Bellemin-Laponnaz and A. Maisse-Francois, *Chem. Eur. J*., 2007, **13**, 3202–3217.
14 C. A. Wheaton and P. G. Hayes, *Chem. Commun*., 2010, **46**, 8404–8406.
15 C. A. Wheaton, B. J. Ireland and P. G. Hayes, *Organometallics*, 2009, **28**, 1282–1285.
16 C. A. Wheaton and P. G. Hayes, *Dalton Trans*., 2010, **39**, 3861–3869.
17 B. J. Ireland, C. A. Wheaton and P. G. Hayes, *Organometallics*, 2010, **29**, 1079–1084.
18 M. D. Hannant, M. Schormann, D. L. Hughes and M. Bochmann, *Inorg. Chim. Acta*, 2005, **358**, 1683–1691.
19 M. Brookhart, B. Grant and A. F. Volpe, Jr., *Organometallics*, 1992, **11**, 3920–3922.
20 J. Sandstrøm, *Dynamic NMR Spectroscopy*, Academic Press, New York, 1982.
21 The calculated barrier is taken as an approximate value due to an inability to achieve full peak separation.
22 A second set of much weaker resonances for the methyl-lactate moiety also consistently appears regardless of temperature. See the experimental details for more information.
23 A. W. Addison, T. N. Rao, J. Reedijk, J. van Rijn and G. C. Verschoor, *J. Chem. Soc., Dalton Trans*., 1984, 1349–1356.
24 P_r is the probability of racemic linkages, where $P_r = 0.5$ for atactic PLA, $P_r = 1$ for completely heterotactic PLA, and was calculated from the formula $P_r^2/2 = [rmr]$. Tetrad sequences were observed in the methine region of homonuclear decoupled ^{1}H NMR spectra. For more details see: (*a*) M. Zell, B. Padden, A. Paterick, K. Thakur, R. Kean, M. Hillmyer and E. Munson, *Macromolecules*, 2002, **35**, 7700–7707; (*b*) M. Chisholm, S. Iyer, D. McCollum, M. Pagel and U. Werner-Zwanziger, *Macromolecules*, 1999, **32**, 963–973.
25 M. Chisholm, N. Patmore and Z. Zhou, *Chem. Commun*., 2005, 127–129.
26 T. Biela, A. Duda and S. Penczek, *Macromol. Symp*., 2002, **183**, 1–10; A. Kowalski, A. Duda and S. Penczek, *Macromolecules*, 1998, **31**, 2114–2122.
27 K. Barral, A. D. Moorehouse and J. E. Moses, *Org. Lett*., 2007, **9**, 1809–1911.
28 A. Ouchi, B. Z. S. Awen, L. Hongxia, Y. Araki and I. Osamu, *J. Photochem. Photobiol. A: Chem*., 2006, **182**, 238–244.
29 T. Tsuritani, H. Mizuno, N. Nonoyami, S. Kii, S. Akao, K. Sato, N. Yasuda and T. Mase, *Org. Process Res. Dev*., 2009, **13**, 1407–1412.
30 M. Kranenburg, Y. E. M. van der Burgt, P. C. J. Kamer and P. W. N. M. van Leeuwen, *Organometallics*, 1995, **14**, 3081–3089.
31 APEX2, Version 2.1-4; Data Collection and Refinement Program. Bruker AXS Inc., Madison, WI, 2006.
32 SAINT-Plus, Version 7.23a; Data Reduction and Correction Program. Bruker AXS Inc., Madison, WI, 2004.
33 G. M. Sheldrick, *SADABS, Area-Detector Absorption Correction, v2.10*, Universität Göttingen, Germany, 1999.
34 G. M. Sheldrick, *Acta Crystallogr*., 2008, **A64**, 112–122.
35 A. L. Spek, *Acta Crystallogr*., 2009, **D65**, 148–155.
36 M. N. Burnett, C. K. Johnson, ORTEP-III: Oak Ridge Thermal Ellipsoid Plot Program for Crystal Structure Illustrations, Oak Ridge National Laboratory Report ORNL-6895, 1996.

